A&A 396, 91–108 (2002)
DOI: 10.1051/0004-6361:20021339

Astronomy & Astrophysics

Binary black holes and tori in AGN

II. Can stellar winds constitute a dusty torus?

C. Zier and P. L. Biermann

Max-Planck Institut für Radiostronomie (MPIfR), Bonn, Auf dem Hügel 69, 53121 Bonn, Germany

Received 25 March 2002 / Accepted 12 September 2002

Abstract. In this second paper, in a series of two, we determine the properties of the stellar torus that we showed in the first paper to result as a product of two merging black holes. If the surrounding stellar cluster is as massive as the binary black hole, the torque acting on the stars ejects a fraction which extracts the binary's angular momentum. After the black holes coalesced on scales of $\sim 10^7$ yr, a geometrically thick torus remained. In the present article we show that a certain fraction of the stars has winds, shaped into elongated tails by the central radiation pressure, which are optically thick for line of sights aligned with them. These stars are sufficiently numerous to achieve a covering factor of 1, so that the complete torus is optically thick. This patchy structured torus is then compared with observations. We find the parameters of such a torus to be just in the right range in order to explain the observed large column densities in AGN and their temporal variations on time scales of about a decade. Within this model the broad absorption line quasars can be interpreted as quasars seen at intermediate inclination angles, with the line of sight grazing the edge of the torus. The half-opening angle of the torus is wider for major mergers and thus correlates with the central luminosity, as has been suggested previously. In this picture the spin of the merged black hole is possibly dominated by the orbital angular momentum of the binary. Thus the spin of the merged black hole points into a new direction, and consequently the jet experiences a spin-flip according to the spin-paradigm. This re-orientation could be an explanation for the X-shaped radio galaxies, and the advancing of a new jet through the ambient medium for Compact Symmetric Objects.

Key words. black hole physics – stellar dynamics – galaxies: active – galaxies: interactions – galaxies: jets – galaxies: nuclei

1. Introduction

Active galactic nuclei (AGN) produce very high luminosities in a very restricted volume, probably via an accretion disk around a massive black hole (BH) in which shear stresses cause matter to sink down in the potential of the BH. These luminous nuclei appear in many different flavours what the unification scheme traces back to a nonspherical symmetry of the nucleus, which is spatially not resolved. Thus the same object looks different if viewed from different directions, leading to various classifications.

Such an AGN we tried to illustrate in Fig. 1 in double logarithmic scales. In the very center is a massive BH of about $10^8\,M_\odot$ with a Schwarzschild radius of about 10^{-5} pc. The observed rapid variation of X-rays on scales of 10^4 s restricts their origin to a volume of about 3×10^{12} m radial extension, which corresponds to the last stable orbit of a black hole of $\sim 3 \times 10^8\,M_\odot$. The X-rays are thought to be generated near the inner regions of the accretion disk, which produces the optical-UV emission in the outer parts, extending to about 10^{-3} pc. On scales up to 0.01 pc the broad emission line region (BLR) is found (Peterson 1993) with line widths corresponding to doppler-broadening with velocities of 1500 up to 30 000 km s^{-1}, probably caused by line emission in clouds moving at these speeds. While these lines are varying on scales of weeks or months, in agreement with the extension of the BLR, the narrow emission lines do not show such variations. Their line widths imply velocities of the order of 1000 km s^{-1} and hence place the narrow emission line region (NLR) at distances up to the kilo parsec scale.

In the infrared (IR) the spectrum shows a bump between 2 μm and 1 mm which is thought to be due to re-radiation by dust in a distance of some parsec from the center (Chini et al. 1989; Sanders et al. 1989) and which is distributed in a toroidal volume around the nucleus, whose symmetry axis is aligned with that of the accretion disk (see Fig. 1).

The observed AGN can basically be divided in two different types, with type 1 objects exhibiting all the features described above. Therefore in these objects the central parts are directly seen without absorbing matter in the line of sight (LOS). On the other hand in sources of type 2, there is no convincing evidence for the directly visible optical-UV emission and the soft X-rays seem to be heavily absorbed (Lawrence & Elvis 1982; Mushotzky 1982). No broad emission lines are detected.

Send offprint requests to: C. Zier,
e-mail: chzier@mpifr-bonn.mpg.de

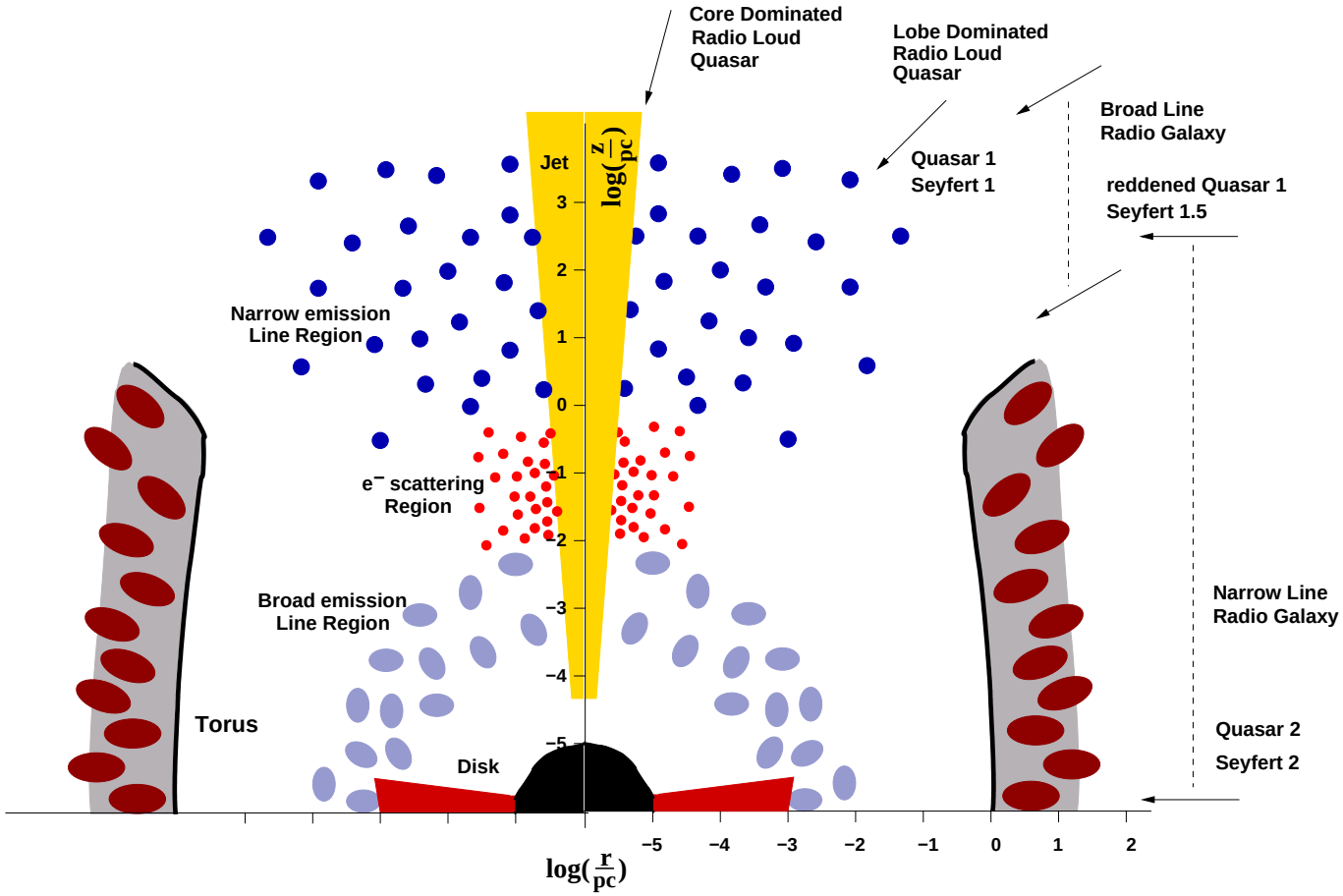

Fig. 1. A sketch of the cylindrically symmetric AGN according to the description in the introduction and to the picture of a patchy torus in AGN, developed in Paper I and this work, is shown. The cut shows the r–z-plane, both axes logarithmically scaled to 1 pc. The basic constituents are the central BH with a surrounding accretion disk, the jet perpendicular to the disk and the torus encircling this configuration. The dark patches in the torus indicate the clouds, made up by stellar winds in our proposed concept. The locations of the BLR, ESR and NLR are shown on the left, as well as the appearance of the nucleus as a function of the angle of the LOS to the jet-axis (on the right). See text for details. Note that a strictly spherical distribution is almost a square box in this diagram.

The unification scheme relates the different types to different orientations rather than intrinsic differences: The type 2 classified nuclei are seen at large inclination angles and consequently the LOS is blocked by the torus so that only the NLR is freely visible and in fact indistinguishable from that in type 1 objects.

Evidence for such obscuring tori is deduced from observed sharply defined conical/biconical nebulae which are suggestive of shadowing (Antonucci 1993 and references therein). The deficit of observed ionizing photons relative to what is needed to ionize the nebulae (Kinney et al. 1991) evidently supports the idea of matter obscuring the central source, which is not obscured at the aspect angles where the ionized nebulae are located. Hence the ionizing photons escape from the center in a cone so that the optical, UV and probably soft X-ray radiation is collimated by the torus, escaping anisotropically through the polar cap regions.

Even stronger support comes from spectrapolarimetry, which reveals in the polarized spectrum of type 2 sources a clear spectrum of type 1 (Antonucci & Miller 1985; Miller et al. 1991). The power-law continuum has the same degree of polarization as the permitted broad lines, which also have normal equivalent width. The degree of polarization is found to be almost wavelength independent. This is interpreted as the reflection of the obscured type 1 continuum by free electrons in the opening of the torus (Antonucci 1993 and references therein). This electron scattering region (ESR) is located somewhere near to the BLR and extends to scales of the height of the torus (Taniguchi & Anabuki 1999), see Fig. 1.

Thus for a small viewing angle with the source being seen almost face on all features of a type 1 spectrum are visible. As the viewing angle increases the LOS finally grazes the edge of the torus and the spectrum becomes reddened. The central regions gradually become more obscured by the torus till the broad lines disappear and the source is classified as type 2 when it is seen near edge on.

As indicated in Fig. 1, there are more criteria than the orientation to distinguish between the different objects, such as the luminosity or the radio properties, with radio loud galaxies having a strong jet streaming along the symmetry axis. For a much more detailed explanation of the unified scheme see for example the reviews by Antonucci (1993), Urry & Padovani (1995) and Wills (1999).

The torus is a very important component in this scheme. To support its vertical thickness previous models either use

magnetic pressure (Lovelace et al. 1998) or radiation pressure (Pier & Krolik 1992b), which faces some problems for low luminosity central sources and smoothly distributed dust. Here we want to further develop our idea, introduced in a previous paper (Zier & Biermann 2001), that this torus is comprised of the winds of stars moving in the potential of a merging binary black hole (BBH), allowing them to maintain the geometrical thickness of the torus.

In that article we simulated the evolution of a stellar cluster under the influence of a massive binary black hole in its center, based on the two widely accepted assumptions that (a) galaxies with an active nucleus harbour a supermassive black hole in their center and (b) that galaxies frequently merge. The results clearly showed that the binary merges on scales of some 10^7 yr due to the ejection of a fraction of stars, if the surrounding stellar cluster is about as massive as the binary, and ensuing emission of gravitational radiation. The stars which remained bound indeed are found to be distributed geometrically in the volume of a thick torus. In this second paper we will investigate, whether such a stellar torus can explain the presence of the ubiquitous torus surrounding apparently all AGN.

The next section will briefly review the constraints put on the properties of the torus by observations.

2. Properties of the torus

Although the current telescopes are not able to spatially resolve the torus in AGN, conclusions could be drawn from observations in various wave bands about the torus' geometry as well as the matter it is made of.

The inner radius

Absorption of the primary optical-UV radiation by dust, which reemits it in the IR, heats the dust to its evaporation temperature (∼1500 K). Inside the evaporation radius dust can not exist and Lawrence (1991) assumed it to be the inner radius of the dusty torus. This radius is about 1 pc, corresponding to the distance where the BBH becomes hard (Milosavljević & Merritt 2001) and what also marks the inner radius of the torus that we obtained in our simulations (Paper I). This value is also in agreement with the inner radius obtained by Krolik & Begelman (1988) from the balance between cloud evaporation by central radiation and inflow by dissipative processes in the torus. In several type 1 AGN variations in the near-infrared (NIR) emission have been observed to lag those at shorter wavelengths (Clavel et al. 1989; Sitko 1991; Baribaud et al. 1992). These time delays place the IR emission source in a distance from the central engine which is consistent with that of optically thin nuclear heated dust at its evaporation temperature.

To explain the bump in the near-infrared in terms of thermal dust emission, a range in the grain temperature is required ($1500\,\mathrm{K} \lesssim T_{\mathrm{dust}} \lesssim 30\,\mathrm{K}$), since isothermal dust close to its evaporation temperature yields a narrower bump than that observed (Sanders et al. 1989; Haas et al. 2000). Thus the torus' temperature has to decrease from the inner edge to its outer regions (Niemeyer & Biermann 1993), but a very thick and compact torus (Pier & Krolik 1992a; Pier & Krolik 1993) is not able to provide such a broad temperature range. Instead a clumpy torus, as suggested by Krolik & Begelman (1988), has the advantage that dust in clouds can survive more easily the strong radiation field, and such a structure of the torus tends to increase the dust temperature in the outer parts (Efstathiou & Rowan-Robinson 1995) where the clouds are exposed to central radiation through gaps in the inner parts of the patchy torus. This seems also most promising to Haas et al. (2000) in order to explain the spectral energy distribution (SED).

Column density N_H

On the basis of X-ray observation lots of evidence has been accumulated that the column density is in the range $10^{22-24}\,\mathrm{cm}^{-2}$ (Mulchaey et al. 1992 for UV-detected Seyfert 2s), or $1–8\times10^{24}\,\mathrm{cm}^{-2}$ (Krolik & Begelman 1988). A more recent study of the X-ray observations of a sample of Seyfert 2 galaxies in the 0.1–100 keV spectral range with *BeppoSAX* has been performed by Maiolino et al. (1998). The sources they studied were selected according to their [OIII] optical emission line flux after correction for the extinction deduced from the Balmer decrements. Hence this sample is thought to be fairly isotropic and avoids a bias against heavily obscured nuclei, as is probably the case in former samples. Maiolino et al. (1998) find all the sources to be absorbed by column densities larger than $4\times10^{23}\,\mathrm{cm}^{-2}$ and most even appear to be thick to Compton scattering with $N_{\mathrm{H}} \gtrsim 10^{25}\,\mathrm{cm}^{-2}$. Hence their results provide further and strong evidence for the unification scheme and indicate that the obscuration in type 2 AGN is probably much higher than deduced from earlier X-ray surveys.

Such high column densities are also deduced from radio data. Conway & Blanco (1995) ascribe the absorption of the broad HI 21 cm line towards the compact radio nucleus of the FR II radio galaxy Cyg A to the obscuration by a torus in about 10 pc distance to a central BH of $\sim10^8\,M_\odot$. Assuming a spin temperature in the range 8000–16 000 K the authors obtain a column density in the range $2–4\times10^{23}\,\mathrm{cm}^{-2}$, in very good agreement with the column $3.75\times10^{23}\,\mathrm{cm}^{-2}$ deduced from previous X-ray spectroscopy by Ueno et al. (1994).

Both, X-ray and radio data show also evidence for a patchy structured torus (Boller et al. 2002; Krichbaum et al. 1998), in agreement with the explanations for the IR range of the previous section.

Opening angle

The observed sharply defined conical/biconical nebulae in some AGN are suggestive of shadowing (Antonucci 1993 and references therein). These ionization-cones, being located in the opening of the obscuring torus and aligned with the inner radio jets (Nagar & Wilson 1999), represent a lower limit of the half opening angle of torus in the range 35° to 50° (Pogge 1989; Wilson et al. 1993; Wilson & Tsvetanov 1994; Macchetto et al. 1994).

Using the statistics of the observed number ratios of Seyfert 1 and 2s (Osterbrock & Shaw 1988; Huchra & Burg 1992; Barthel 1989; Willott et al. 1999) a half-opening angle of

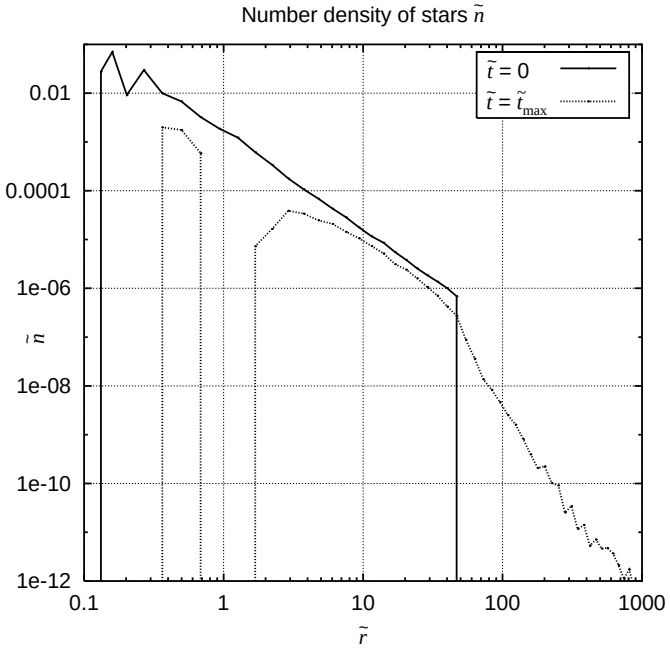

Fig. 2. The stellar number density distribution is shown at the beginning ($\tilde{t} = 0$) and end ($\tilde{t} = \tilde{t}_{max}$) of the simulation. Finally, at $\tilde{t}_{max}$, the bound star distribution follows a powerlaw with index -4 in the heated region ($\tilde{r} \gtrsim 50$), while an index ~ -2 is maintained in the range $10 \lesssim \tilde{r} \lesssim 50$. The inner parts are scoured out due to ejection of stars by the binary, and a maximum emerges at $\tilde{r} \approx 3$, showing the torus-like configuration the stars assume. For $\tilde{r} \lesssim 0.7$ a cusp of stars bound to M_1 only is left. $\tilde{r}$ is normalized to 1 pc and $\tilde{n}$ such that the area underneath the solid line is 1.

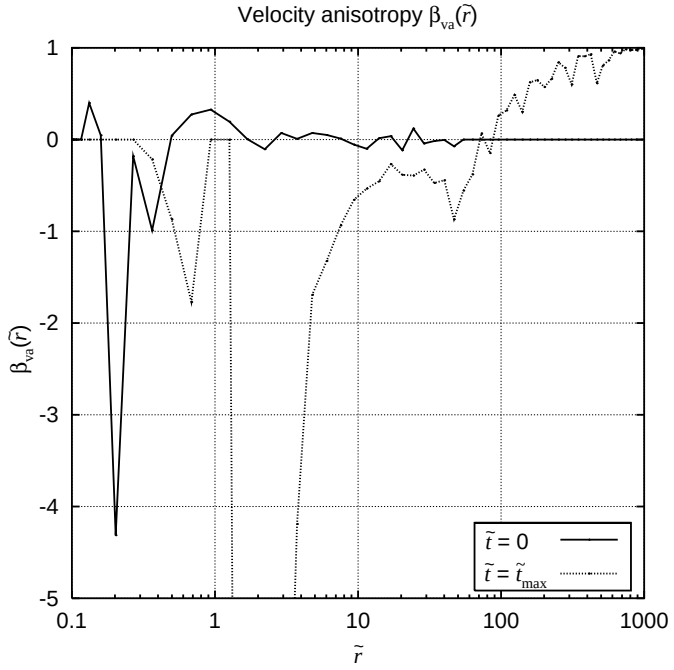

Fig. 3. The initial conditions ($\tilde{t} = 0$) of the star cluster have been set so that the velocity anisotropy $\beta_{va} = 1 - \frac{\langle \tilde{v}_\phi^2 \rangle - \langle \tilde{v}_\theta^2 \rangle}{2\langle \tilde{v}_r^2 \rangle}$ is neither radially (≥ 1) nor tangentially (≤ 1) anisotropic. At $\tilde{t} = \tilde{t}_{max}$ the velocity anisotropy of the bound stars is a strongly increasing function of the radius. In the range $r \lesssim 50$ they are tangentially anisotropic, while in the heated region ($r \gtrsim 50$) the stars are moving on radially anisotropic orbits.

the torus in the range 30°–60° is obtained. This matches very well the angles of the ionization-cones inside the opening of the torus.

Covering factor

According to the opening angle of the torus, it screens a considerable fraction of the solid angle, seen from the central source, and is geometrically thick. Blocking the view to the nucleus in type 2 AGN, the torus, if comprised of individual clouds, must be optically thick for most of the lines of sight penetrating it. Thus the clouds constituting the torus must achieve a covering factor of about one, if a single cloud is optically thick, and more otherwise.

Hence the observations demand a clumpy-structured torus with an inner radius of about 1 pc, that is optically and geometrically thick with a half-opening angle of ∼45° and therefore has a covering factor of order unity.

3. Kinematics and density distribution of the stars

Our simulation of a stellar distribution in the potential of the binary (discussed in detail in Paper I, Zier & Biermann 2001) has been performed for three different mass-ratios of the BHs ($q = 1, 10, 100$), with

$$q = \frac{M_1}{M_2},$$

where $M_1 \geq M_2$, always. While we focused on the ejected fraction of the stars in that article we will discuss in this section the bound population. For clarity we first briefly summarize just a few results from Paper I, using a mass-ratio of the BHs of $q = 1$.

3.1. Dynamics of the bound stars

In order to write the equations in their dimensionless form, denoted by a tilde " ˜ " on top of the quantities, we used the following normalization parameters:

$$r_0 = a = 1\,\mathrm{pc},$$
$$t_0 = \sqrt{\frac{r_0^3}{G(M_1 + M_2)}},$$
$$L_0 = \frac{ma^2}{t_0}.$$

The semi-major axis of the BBH is denoted by a, and for the mass of a typical star m we used one solar mass.

During the simulation the initial singular isothermal sphere evolves finally into a distribution which is depleted in the inner regions (see Fig. 2). The stellar density peak at about $\tilde{r} = 0.5$ is made up by a fraction less than 0.4% of the final distribution and is bound to the primary black hole only. Since we expect this cusp to be much shallower if we would have taken into account the shrinking of the binary in the calculations, we will not address it further in our discussion.

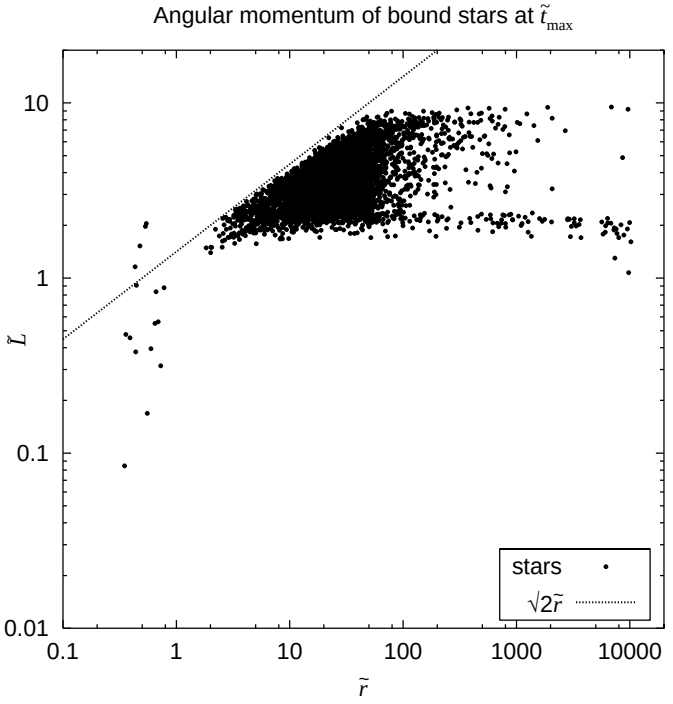

Fig. 4. Plotting the angular momentum $\tilde{L}$ versus the distance $\tilde{r}$ at $\tilde{t}_{max}$ shows all stars to respect the upper limit indicated by the dotted line. Only some stars in the cusp region ($\tilde{r} < 1$) have larger angular momenta, because they are bound to one BH only, with the other perturbing their orbits, so that the assumption of a point-mass potential does not apply at these small distances. For $\tilde{r} \gtrsim 50$ two populations can be distinguished, one clustering around $\tilde{L} \approx 2$ (heated stars) and the other having an upper limit of $\tilde{L} \approx 10$, fading towards smaller values (relaxation process). See text for details.

After a gap in a distance corresponding to the radial distance of the secondary black hole to the center, the density increases again and peaks at $\tilde{r} \sim 3$. In the range $10 \lesssim \tilde{r} \lesssim 50$ the density follows the initial powerlaw of the isothermal sphere ($\tilde{n} \propto \tilde{r}^{-2}$) and for radii bigger than the outer limit of the initial distribution ($\tilde{r} \gtrsim 50$) approximates a powerlaw with index -4.

In Paper I we showed that the stars with small angular momenta, i.e. small pericenters, get close to the orbit of the secondary black hole where they are strongly interacting with both BHs, so that they become ejected. Only stars moving on orbits with sufficiently large pericenters ($\tilde{r}_- \gtrsim 2$) can remain in the central regions. The smaller their radii, the more they are tangentially anisotropic (see Fig. 3) and the less eccentric are their orbits. A fraction of the stars which are interacting with the BHs will be heated to larger distances and stays bound to the binary instead of becoming ejected. Such stars did not gain as much energy as the ejected ones and contribute to the distribution at distances larger than the extension of the initial distribution, which terminates at $\tilde{r} = 50$ (see Fig. 2).

In addition to these stars we will find in this region ($\tilde{r} \geq 50$) also those which happen to be close to their pericenters at the very beginning of the simulation due to the choice of the initial conditions. As time proceeds they are moving on their orbits without being noticeably affected by the secondary BH, whose perturbation to a point-mass potential is negligible at large distances. Thus, keeping their energy and angular momentum nearly conserved, these stars diffuse into the outer regions ($\tilde{r} \geq 50$). The expansion of the initial distribution is just a process of relaxation and would have occurred also in a point-mass potential. Thus the region at $\tilde{r} \geq 50$ is partly populated by stars which did not interact with the binary.

Both these populations can be clearly distinguished in Fig. 4, where we plotted the angular momentum versus the radius for each single star at the end of the simulation. For $\tilde{r} \gtrsim 50$ one population is clustering around $\tilde{L} \approx 2$ and the other having an upper limit at $\tilde{L} \approx 10$, fading towards smaller angular momenta. Both are extending to radii of about 10^4, with the former population being more pronounced at such big distances.

In a point-mass potential the energy reads in dimensionless units

$$\tilde{E} = \frac{\tilde{v}_r^2}{2} + \frac{\tilde{L}^2}{2\tilde{r}^2} - \frac{1}{\tilde{r}}\,, \tag{1}$$

with the maximum energy of a bound star just below zero. To maximize the angular momentum, all its kinetic energy is assumed to be stored in tangential motion so that $\tilde{v}_r = 0$. Solving now for the angular momentum gives

$$\tilde{L} < \sqrt{2\tilde{r}} \tag{2}$$

as the upper limit for bound stars. This power law with index $1/2$ is indicated in Fig. 4 by the dashed line.

However, the nature of the two populations at $\tilde{r} \gtrsim 50$ can be understood easily if we calculate the maximum possible angular momentum for the stars as function of their initial pericenter. In dimensionless form this is

$$\tilde{r}_- = \frac{\tilde{L}^2}{1+\epsilon}\cdot \tag{3}$$

In order to obtain an upper limit for the angular momentum of the diffused population, we assume that some stars at $\tilde{r} = 50$ are initially at their pericenter and move on highly eccentric orbits ($\epsilon \to 1$). Solving then Eq. (3) for $\tilde{L}$ yields an upper limit of

$$\tilde{L}_{\rm lim} = \sqrt{2\tilde{r}_-} = 10\,. \tag{4}$$

If we use for the initial pericenter $\tilde{r}_- = 2$ instead of 50 we obtain $\tilde{L}_{\rm lim} = 2$. This clearly shows that the stars at $\tilde{r} \gtrsim 50$, whose angular momenta tend to 10, initially have been close to $\tilde{r} = 50$ and thus diffused into this region. On the other hand the stars with angular momenta $\tilde{L} \approx 2$ had initial pericenters close to the radius of the orbit of the secondary BH. Here they strongly interacted with the BBH before they were heated to distances up to 10^4 (Fig. 4). The heated stars in fact are very similar to the ejected ones which have been discussed in detail in Paper I. Their velocity distribution is also radially anisotropic ($\beta_{\rm va} > 0$, see Fig. 3) and they are moving on highly eccentric orbits. The heated stars just did not gain sufficient energy as to escape from the binary.

This can be confirmed by computing the maximum distance a star can travel, when it is moving at escape velocity, $\tilde{v}_{\rm esc} = \sqrt{2/\tilde{r}}$. If we integrate $\tilde{v}_{\rm esc}$ with respect to time from the beginning till the end of the simulation ($\tilde{t}_{\rm max} = 5 \times 10^5$) this distance is

$$\tilde{r}_{\rm max} = \left(\frac{3}{\sqrt{2}}\,\tilde{t}_{\rm max} + \tilde{r}_{\rm i}^{3/2}\right)^{\frac{2}{3}} \approx 10^4\,, \tag{5}$$

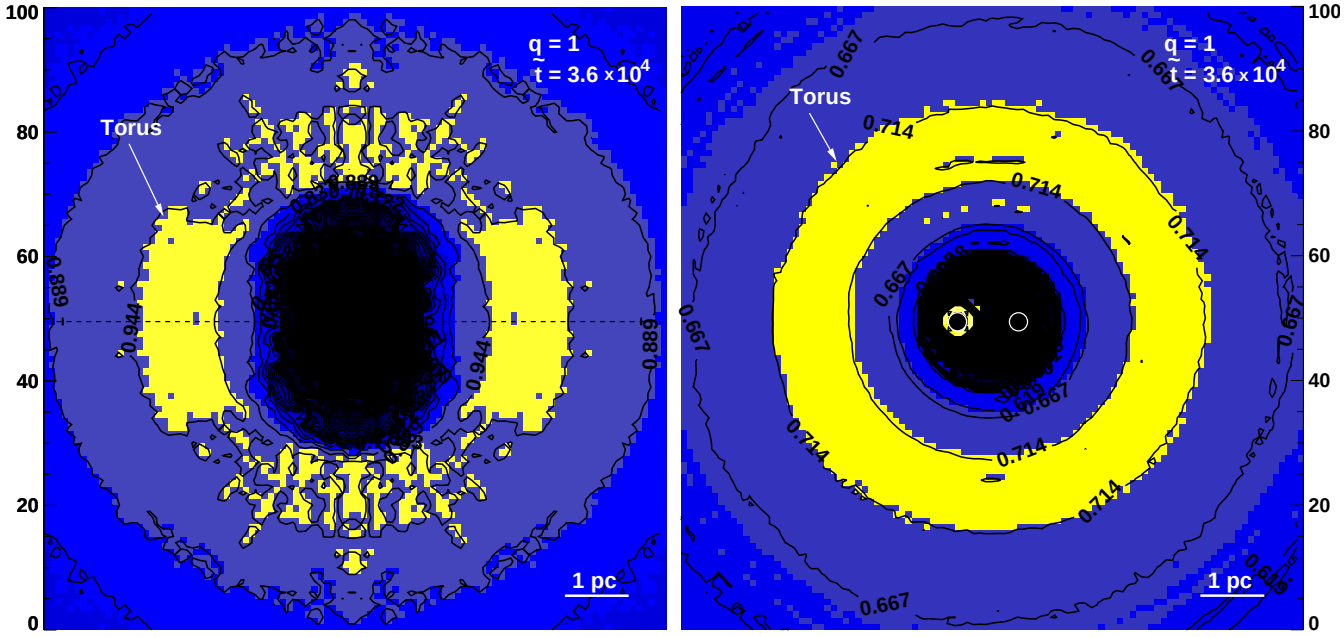

Fig. 5. Cuts through the stellar density in the comoving frame are shown with contours scaled logarithmically. The right panel displays the equatorial plane (BHs marked by black spots). Perpendicular to it the $x = 0$-plane is shown (left panel), with the y-axis drawn as dashed line, so that the BHs are in front and behind the paper-plane. The initial distribution is a Gaussian and the mass-ratio is 1. After initially stars close to the orbits in 0.5 pc distance from the center are ejected and the polar regions are depleted, finally a torus emerges in the equatorial plane at $r \sim 3$ pc. An expanded version of this diagram for the mass-ratio 10 is shown in Paper I.

corresponding to the largest radii in Fig. 4. For the initial radius $\tilde{r}_\mathrm{i}$ we have inserted values ranging from 0 to 50, but since the first term in the brackets dominates the expression it does not make a difference whether the stars started in the center or from the edge of the initial distribution.

The bound stars in the intermediate range eventually assume a torus-like structure as is shown in Fig. 5, which is taken from Paper I. This plot displays cuts through the 3-dimensional stellar density distribution in the comoving frame of the binary after about 10^7 yr when the BHs have merged. The right panel shows the equatorial plane ($z = 0$) with the BHs marked by the black points, M_1 to the right. The slice in the left panel is perpendicular to the equatorial plane and contains the $x = 0$-plane, with the y-axis indicated by the dashed line. While the stars initially have been distributed according to a Gaussian, the central parts have been scoured out and a torus in the equatorial plane of the binary with a radius of about 3 pc is left. The basic topology of the final density distribution can be understood in physical terms, when we consider the torque exerted by the two black holes on an orbiting star. Figure 3 in Paper I shows of the normalized torque the component $\dot{\tilde{L}}_{z,1}/\tilde{r} = \tilde{r}\ddot{\phi}\sin^2(\theta)$ relative to the z-axis of the BBH as a function of time for different angles θ between the rotation axis of the BBH and the symmetry axis of the star's orbit. The bigger the angle θ is (i.e. for orbits through the polar regions), the more is the star's trajectory disturbed by the influence of the two BHs. The cumulative effect of these large excursions in the polar cap regions deplete the stellar population, leaving a torus behind.

The toroidal structure which the bound population assumes once the BHs are merged is confirmed also by the kinematics of the stellar distribution. The tangential velocity components of a single star moving on an orbit which is inclined by the angle θ to the equatorial plane are

$$\tilde{v}_\phi = \tilde{v}_\mathrm{t}\cos\theta_v$$
$$\tilde{v}_\theta = \tilde{v}_\mathrm{t}\sin\theta_v\,,$$

where θ_v is the angle enclosed by the binary's rotation axis and the velocity-vector $\boldsymbol{v}$ of the star. Thus the total tangential velocity component is $\tilde{v}_\mathrm{t} = (\tilde{v}_\phi^2 + \tilde{v}_\theta^2)^{1/2}$. For stars constrained to a torus-like volume, as shown in Fig. 5, we expect their azimuthal velocity component $\tilde{v}_\phi$ to exceed the polar component $\tilde{v}_\theta$. This is verified in Fig. 6, where we have plotted the mean square of each velocity component versus the radius: At the inner edge of the torus between 1 and 2 pc distance (Figs. 2 and 5) the mean square of the azimuthal component is a factor of about 10 larger than $\langle\tilde{v}_\theta^2\rangle$. With increasing radius both components approach each other and at about 8 pc they are almost indistinguishable.

4. Stellar winds comprising a patchy torus

Now that eventually the bound stars indeed constitute a torus-like distribution which is geometrically thick, just as required by the unification scheme, we may ask about the effects of this structure on the radiation emitted from the center. Of course the stars alone are not able to obscure this radiation, since at a distance of about $r = 3$ pc a number of order of at least $(r/R_*)^2 \approx 10^{12}$ stars would be required to achieve a covering factor of order unity, using giant stars with a radius of 10^{11} m. But if there is a sufficiently large number of stars in the torus

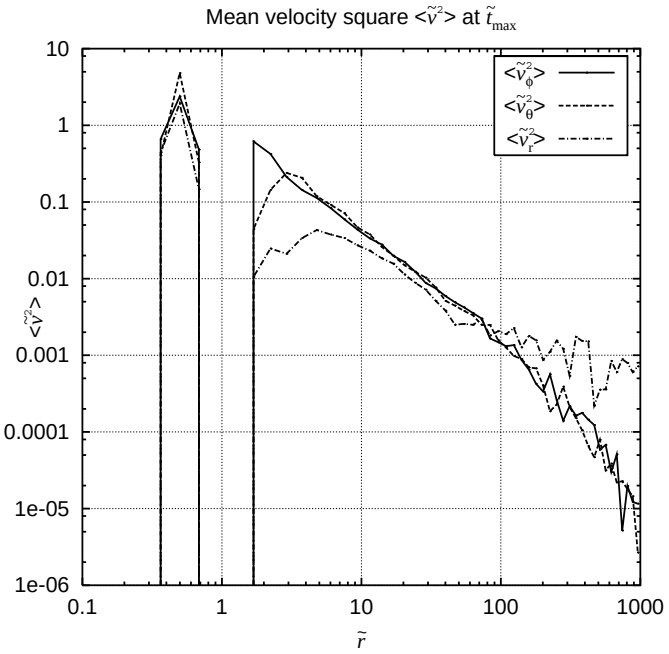

Fig. 6. The mean of the squares of the velocity components in spherical coordinates are displayed at $\tilde{t}_{max}$. In the range of the initial distribution ($\tilde{r} \leq 50$) both tangential components exceed the radial one, while at larger distances it is just the opposite, in accordance with Fig. 3. In the range from the inner edge of the torus at $\tilde{r} = 1$ to the maximum of the number density at $\tilde{r} = 3$ (Fig. 2), the azimuthal component is larger than $\langle \tilde{v}_\theta^2 \rangle$, in favour of the toroidal distribution of the stars. At larger distances these components become indistinguishable.

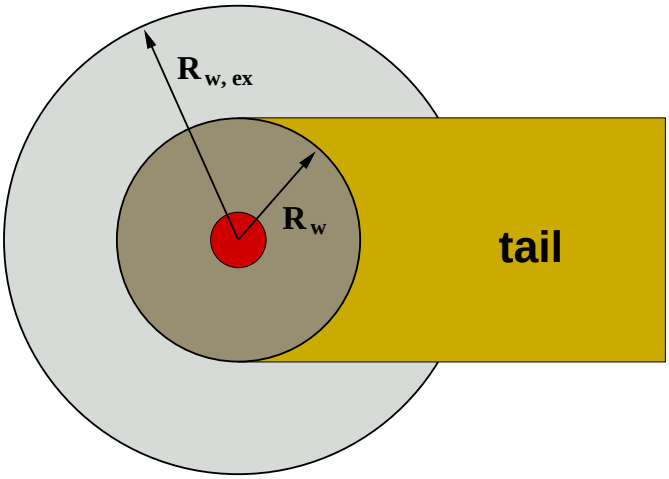

Fig. 7. This sketch illustrates how the radiation pressure of a strong source, located in a large distance d ($d \gg R_{w,ex}$) left from the star, shapes the wind into a comet-like tail, pointing radially away from the source. The radius of the cross-section area of the wind is R_w, and $R_{w,ex}$ denotes the radius of a freely expanding wind.

with dense winds which absorb a significant fraction of the central radiation, the complete torus might be opaque. To get an estimate of the optical depth and density of the torus we have to examine its constituents, the stars and their winds, more closely.

Solar type stars are not appropriate for the obsuration of the AGN, since their winds are too weak. But there are various other stars which can account for the obscuration and which we will call "obscuring stars" (OS) in the following. Using evolutionary tracks, Young et al. (1977) showed that the total fraction on the giant branch in a cluster ranges between 1% and 2% for an interval 1 to 5 billion years after coeval star formation. In a first paper Shull (1983) assumed a dense stellar cluster to consist of two components, one evolved component of red giants ($1\,M_\odot$, $100\,R_\odot$) comprising 1% of the stars, and a main-sequence component. In a later paper (Voit & Shull 1988) the fraction of supergiants in a thermal cluster was assumed to comprise only 0.01%, giants ($1\,M_\odot$, $10\,R_\odot$) 1% and the rest of the cluster to be made up by main-sequence stars. This would be only a small fraction with stars having mass-loss rates of typically $10^{-5}\,M_\odot$/yr. On the other hand the observed $FWHM$ within the inner 160 pc of both Hα and [N II] and the equivalent width of the Ca II lines are indicating the presence of an important population of red supergiants in the nucleus of NGC 6951 (Pérez et al. 2000). The current understanding of stellar winds is based on observations in the solar neighbourhood and so far there are no results concerning the possible effect of the intense radiation of the AGN on the wind structure. Thus stars in AGN might be very different from stars in the outer galaxy (Alexander & Netzer 1994; Alexander & Netzer 1997). There are theories that the conditions in AGN are likely to enhance the mass-loss rate of irradiated stars near the center (Edwards 1980; Shull 1983; Voit & Shull 1988; Tout et al. 1989). While this radiation might not significantly increase the mass-loss rate (Voit & Shull 1988), Biermann (1989) and Stecker et al. (1991) suggested a significant neutrino flux in AGN which may transform low-mass stars into red giants (MacDonald et al. 1991). Since we consider the the torus to be a consequence of two merging galaxies with central massive black holes, besides stars we also expect big amounts of gas to be brought to the center, and therefore an enhanced formation rate of young stars with high mass-loss rates. This is supported by Pérez et al. (2000), who find evidence that star formation occurs in bursts and continuously inwards to the nucleus from a 5 arcsec radius in NGC 6951, and Oliva et al. (1995), who investigated red supergiants as starburst tracers in galactic nuclei. They find a large value of L_H/M in NGC 1068, confirming the presence of a decaying starburst in the central regions ($R < 3''$). We will condense the previous arguments into the simple assumption, that the obscuring stars with strong winds amount to a fraction of 1% of the central cluster.

The radiation pressure of a bright central source limits the wind-radius in its extension and will shape it into an elongated tail, pointing radially away from the central source. This is illustrated for one star in Fig. 7. The large light-grey shaded circular area represents the freely expanding wind of the star in its center. The dark-grey area shows the smaller extension of the wind, limited by a central source far left from the star, which shapes the wind into a comet-like tail.

Such bending of the wind into a tail by radiation pressure can be deduced from a crude and simple estimate. According to Mathis et al. (1977), Graphite with its evaporation temperature $T_{evap} \sim 1500$ K is the major contributor to the extinction of the radiation outside the evaporation radius r_{evap}.

This corresponds to the distance from the center, where the absorption of the central UV radiation by dust grains equals the rate at which it is reradiated as thermal IR radiation, such that the equilibrium temperature is the evaporation temperature. The absorption efficiency of the grains in the IR is much smaller than in the optical/UV, so that the reemission in the near IR (NIR) must be optically thin. Barvainis (1987) approximated the IR-absorption efficiency by a powerlaw ($Q_\nu \propto \nu^\gamma$) with the index in the range 1 to 2. This yields a spectrum with a considerably narrower bump at 2 μm than is observed (Sanders et al. 1989; Haas et al. 2000) and which corresponds to the optically thin emission peak of the hottest grains at a temperature $T_{\rm gr} \approx 1500\,{\rm K}$. Hence, any model which seeks to explain the NIR bump in terms of thermal dust emission requires a range in the grain temperature. This is naturally included in our model, since the heated dust will be in equilibrium at different temperatures at different distances from the central radiation source. For the grain temperature as function of the distance r to the center Barvainis (1987) obtained

$$T_{\rm gr} = 1650 \left(\frac{L_{\rm uv,46}}{r_{\rm pc}^2} \right)^{\frac{5}{28}} {\rm e}^{-5\tau_{\rm uv}/28}\,{\rm K}\,, \tag{6}$$

with $\tau_{\rm uv}$ as the optical depth of dust in the UV and $L_{\rm uv,46}$ being the central UV luminosity in units of $10^{46}\,{\rm erg/s}$. $r_{\rm pc}$ is the distance normalized to 1 pc. Using $T_{\rm evap}$ for the grain temperature and solving this equation for r gives the evaporation radius

$$r_{\rm evap} = 4.05\, L_{\rm uv,46}^{1/2} T_{\rm evap,3}^{-14/5}\,{\rm pc}\,, \tag{7}$$

where $T_{\rm evap,3}$ denotes the evaporation temperature in units of 1000 K.

Assuming a star to be located inside $r_{\rm evap}$ where the Thomson cross-section $\sigma_{\rm th}$ applies, its wind extension can be calculated using the same Ansatz as for the Eddington limit, i.e. equating the force of the central radiation acting on the wind particles with the kinetic force of the wind,

$$\frac{L_{\rm uv}\sigma_{\rm th}}{4\pi r^2 c} = \frac{m_{\rm p} v_{\rm w}^2}{R_{\rm w}}. \tag{8}$$

With typical values of red giants for the wind velocity $v_{\rm w}$ (Knapp & Morris 1985; Winters et al. 1994; Hoefner et al. 1996) this equation can be solved for the extension of the wind,

$$R_{\rm w} \approx 1.2\times10^{-3} \left(\frac{r}{2\,{\rm pc}} \right)^2 \left(\frac{v_{\rm w}}{10\,\frac{\rm km}{\rm s}} \right)^2 \left(\frac{L_{\rm uv}}{10^{46}\,\frac{\rm erg}{\rm s}} \right)^{-1} {\rm pc}. \tag{9}$$

This is only a very rough estimate. In the following we are seeking for a more robust value of the wind radius, which is based on confirmed limits set by observations. As discussed in Sect. 2, these tell us that the torus is optically thick and the covering factor of its constituents, the stars, is about one. Therefore the number density of obscuring stars, integrated along the radial extension of the torus, yields a surface density of the number of stars ($\Sigma_{\rm os}$) which has to equal the inverse of the cross-section area of the stellar winds, i.e.

$$\Sigma_{\rm os} = \frac{1}{\pi R_{\rm w}^2}. \tag{10}$$

$R_{\rm w}$ denotes the radius of the cross-section area of the stellar wind perpendicular to its radial extension. To calculate the surface density we employ the number density profile of the singular isothermal sphere that we have already used in Paper I ($n \propto r^{-2}$), and which has not been much altered by the merging-process of the two BHs (Fig. 2). With n_0 being the number density in the distance $r_0 = 1$ pc we can write

$$n(r) = n_0 \left(\frac{r_0}{r} \right)^2. \tag{11}$$

Integrating this density from the inner to the outer radius of the torus ($r_{\rm in}$ and $r_{\rm out}$ respectively) gives the surface density:

$$\Sigma_{\rm os} = \int_{r_{\rm in}}^{r_{\rm out}} n(r){\rm d}r = \frac{n_0 r_0^2}{r_{\rm in}} \left(1 - \frac{r_{\rm in}}{r_{\rm out}} \right). \tag{12}$$

To determine the number density n_0, we have to calculate the number of obscuring stars in the torus, which is the fraction 0.01 of the bound stars $N_{\rm bn}$. Integrating the number density in Eq. (11) over the volume of the torus gives us the number of obscuring stars $N_{\rm os}$:

$$\begin{aligned} N_{\rm os} &= \int_0^{2\pi} {\rm d}\phi \int_{\theta_{\rm trs}}^{\pi-\theta_{\rm trs}} \sin\theta\,{\rm d}\theta \int_{r_{\rm in}}^{r_{\rm out}} n(r) r^2 {\rm d}r \\ &= 4\pi \cos\theta_{\rm trs} n_0 r_0^2 (r_{\rm out} - r_{\rm in})\,, \end{aligned} \tag{13}$$

where $\theta_{\rm trs}$ is the half-opening angle of the torus. Solving this equation for n_0 and applying it to Eq. (12), the wind radius is obtained with the help of Eq. (10),

$$R_{\rm w} = \left(\frac{N_{\rm os}}{4\cos\theta_{\rm trs} r_{\rm in} r_{\rm out}} \right)^{-\frac{1}{2}} \approx 1.8\times10^{-3}\,{\rm pc}\,. \tag{14}$$

For the parameters we assigned in the last step the values for the case of a mass-ratio $q = 1$: the inner radius is $r_{\rm in} = 1\,{\rm pc}$ (see Paper I and Sect. 2), and 5 pc is used for the outer radius since the density drops quickly with increasing distance. The half-opening angle is 60° (see Fig. 5) and $N_{\rm os} = 0.01\,N_{\rm bn}$, with $N_{\rm bn} = 3\times10^8$ being a little more than the minimum of stars required to allow the BHs to merge (2.3×10^8). The wind radius computed in Eq. (14) is in very good agreement with our crude estimate in Eq. (9) and thus confirms the assumptions we made to obtain it.

Such a wind has to be optically thick ($N_{\rm H} \simeq 10^{24}\,{\rm cm}^{-2}$) for all line of sights through its cross-section. We assume, that the density of such a tail, if projected along its radial extension, yields a constant surface density. Therefore the mass in the wind can be estimated to be of order of

$$M_{\rm w} = \pi R_{\rm w}^2 N_{\rm H}\, m_{\rm p} \approx 8.4\times10^{-2}\,M_\odot\,. \tag{15}$$

The final picture of our model for the torus is illustrated (not to scale) in Fig. 8. The sum of the winds of the obscuring stars, shaped into elongated tails by the central radiation pressure, form a patchy, optically and geometrically thick torus. For an observer whose line of sight (LOS) is aligned with such a wind, the nucleus is obscured and only radiation scattered into the LOS will be detected. Since the number density of the stars decreases for smaller inclination angles between the LOS and the symmetry axis of the torus, the probability to observe the

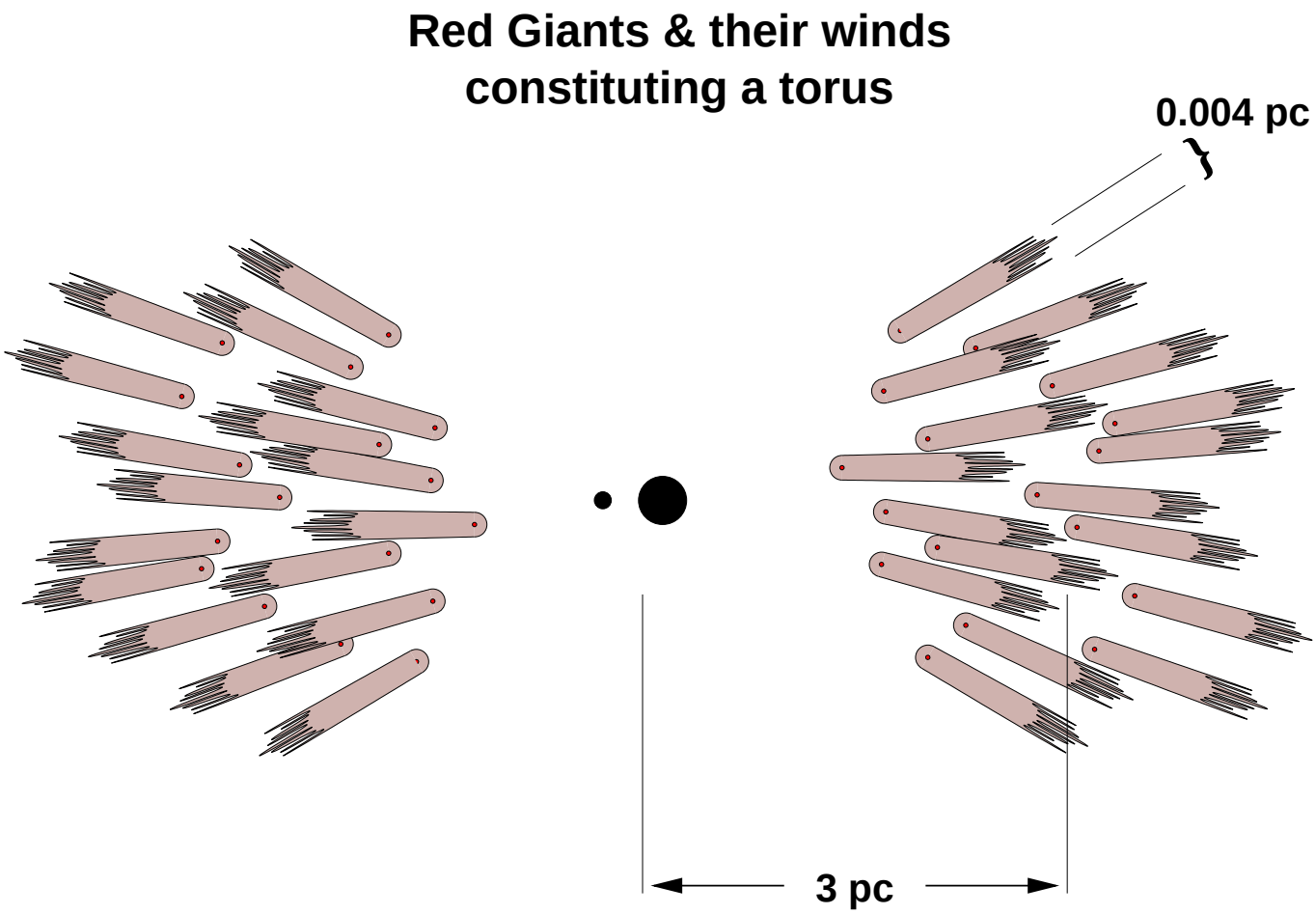

Fig. 8. This picture shows (not to scale) a sketch of the obscuring stars and their winds comprising a torus with the BBH in its center. In this cross-section through the torus, whose density peaks in about 3 pc distance, the obscuring stars are indicated by the small dots. They are surrounded by their winds, which are elongated by the central radiation into comet-like tails (shaded) with a lateral extent of about 0.004 pc. The central radiation source with the BBH is marked by the two BHs in the center. An observer with the LOS close to the edge of the torus might see the center through a gap directly, while the view of an observer with his LOS close to the equatorial plane of the BHs is probably blocked by the winds of at least one obscuring star.

nucleus unobscured, or only partially covered, through a gap in the torus, increases. Such gaps will be continuously opend and closed due to the motion of the stars. According to our prerequisites Eq. (10) is satisfied and consequently the complete torus is optically thick on average.

With the number of obscuring stars and the mass contained in their winds we can estimate the order of magnitude of the dust-mass which is confined to the stellar winds outside the evaporation radius. The relation between the dust and gas mass is given by

$$m_{\rm d} n_{\rm d} = 1.4 Z_{\rm d} m_{\rm p} n_{\rm H}\,, \tag{16}$$

where $m_{\rm d}$ and $m_{\rm p}$ denote the mass of a dust grain and the proton mass respectively. The number-densities are accordingly given by $n_{\rm d}$ and $n_{\rm H}$ with $Z_{\rm d}$ as the dust-to-gas mass-ratio. Integrating over the volume of the wind yields $M_{\rm d} = 1.4\ Z_{\rm d}\ M_{\rm gas}$. This is substituted in $M_{\rm w} = M_{\rm d} + M_{\rm gas}$ and solved for the dust mass:

$$M_{\rm d} = \frac{1.4\ Z_{\rm d}}{1 + 1.4\ Z_{\rm d}} M_{\rm w} \approx 1.2 \times 10^{-4}\ M_\odot\,. \tag{17}$$

In the last expression we used the wind mass of Eq. (15) and for the dust-to-gas mass-ratio $Z_{\rm d} \approx 10^{-3}$ (Hoefner et al. 1996). Multiplying this dust mass with the number of obscuring stars needed to maintain a covering factor of 1 ($N_{\rm os} = 3 \times 10^6$) gives the total dust mass contained in the wind of the obscuring stars,

$$M_{\rm d,total} = M_{\rm d} N_{\rm os} = 350\ M_\odot. \tag{18}$$

This is about a factor of 10 more than the minimum values given by Sanders et al. (1989), which are required to fit the spectra. Within spheres of the radii 1 pc and 10 pc they obtain for the minumum of dust amounts 0.2 $M_\odot$ and 20 $M_\odot$ respectively, using for the grains the parameters given in Mathis et al. (1977) and Biermann & Harwit (1980). If all grains within the given radius are larger than $\sim$1 μm, or are not directly exposed to UV radiation, the required dust mass is $\sim$10 times higher, in good agreement with Eq. (18). Such shielding of the outer regions of the elongated winds by the inner parts is a natural consequence of our model and diminishes the UV irradiation of the outer parts of the wind. Also, due to a covering factor of about 1 it is likely that the wind of a star is covered by that of another one at smaller distances to the central source.

The picture which emerges from our simulations and the results is the following: if a BBH is surrounded by a stellar population of comparable mass, the stars which are ejected in violent interactions with the BHs are able to carry away enough angular momentum of the binary so that it hardens till finally gravitational radiation dominates the shrinking process of the BHs (Paper I). These eventually coalesce after about 10^7 yr, having spent most of the time in the range when the ejection of stars dominates the hardening. On the other hand for the same number of initial stars there are enough left which are bound to the binary and form a torus-like distribution which peaks in about 3 pc distance. In this section we could show that the amount of obscuring stars in the remaining cluster is sufficiently large so that their winds achieve a total covering factor of about 1. These winds are optically thick. Thus the patchy torus as a total is geometrically as well as optically thick so that our model can indeed account for a dusty torus in the center of AGN, as is demanded by the unification model.

4.1. Relativistic boosting

Within the solid angle of a relativistc jet, the radiation is boosted and so the flux density of the approaching radiation, seen under an angle θ to the velocity of the moving source, scales as (Rybicki & Lightman 1979; Longair 1981)

$$S = D^{3-\alpha} S',$$

with α being the spectral index and D the relativistic Doppler factor

$$D = \frac{1}{\gamma(1 - \beta\cos\theta)}.$$

The primed quantities refer to the comoving frame of the source. Thus, for an index $\alpha \sim -1$, the observed flux density depends on the Doppler factor to the power of four. Half of the radiation is emitted in a cone of half-opening angle $\theta \simeq 1/\gamma$, if $\gamma \gg 1$, and thus is strongly beamed. In this limit ($\gamma \gg 1$) we have $D \approx \gamma$ and the luminosity in the cone is a strongly increasing function of γ. If we assume the luminosity L to scale in the same way as S with γ, it increases very strongly in the beaming cone (i.e. by a factor of 10^4 for $\gamma = 10$ and $\alpha = -1$). Consequently, according to Eq. (9), the extension of the winds of the obscuring stars, exposed to the strong beamed radiation, is negligible and the covering factor in this region tends to zero. This means that within the beaming cone, and if the jet is precessing, within the cone of precession, the emission from the jet frees the polar cap regions from obscuring clouds, and therefore supports the toroidal structure of the central absorber.

4.2. Lifetime of the torus

After the merger of the BBH is completed, the toroidal structure of the stellar distribution will not collapse and is stable (Paper I). Therefore the torus will decay on timescales of the lifetime of its constituents, the obscuring stars (i.e. red supergiants and bloated super-giant stars) or has to be replenished with stars from outside. Because after the merger no torque acts anymore on the stars, the stars fed to the torus from larger distances would have to be accreted in an axi-symmetric way to maintain the torus-like shape of the circum-nuclear stellar distribution. The jet-outflow probably helps to keep the polar-cap regions free from stars. But probably the rate of stars accreted to the torus will decrease with time, as the outer regions, stirred up by the merger, will relax with time.

Hence, unless the required number of obscuring stars is not maintained for a longer time by the evolution of the other stars in the cluster, the life-time of the torus will be of comparable order as the time needed by the BHs to coalesce from the distance where a torus emerged due to their torque acting on the surrounding stars. Once the binary has become hard ($a \sim 1$ pc), the BHs merge on scales of about 10^7 yr (Paper I).

In the next sections we present implications and predictions of the proposed model.

5. Jet-flip due to spin-flip of the primary BH

As we have already mentioned in Paper I, we expect the merger of two galaxies of comparable size to result in a galaxy of early type, i.e. of elliptical shape (e.g. Tinsley & Larson 1977; Biermann & Shapiro 1979; Farouki & Shapiro 1982). The spiral structure the parent galaxies might have had will not survive such an event. On the other hand, radio-loud AGN so far have not been found in spiral host-galaxies, what suggests radio-loud galaxies to be the product of one or more major mergers. Since observations show that spectra from AGN in the range from IR to X-rays, dominated by emission from an accretion disk, are basically the same (Sanders et al. 1989), Wilson & Colbert (1995) argue that the distinction between radio-loud and radio-quiet AGN is due to the different spins of the central supermassive BHs. They propose radio-loud objects to harbour a fast spinning super-massive BH as result of a recent major merger, whith the assumption of non-rotating BHs in the parent galaxies. The time scales we obtained for the merging of the BHs are considerably smaller than a Hubble-time, in agreement with such a model.

But what happens, if one of the progenitor galaxies has a fast spinning BH in its center with a powerful radio-jet aligned with it's spin? The situation before such BHs merge is depicted in the left panel of Fig. 9. The spins of both BHs and the orbital angular momentum of the BBH are randomly oriented to each other, because the merger of both galaxies does not proceed in a favored plane relative to that of the galaxies. While the secondary BHs spin is assumed to be negligible, we adopt for the primary BH a spin that is sufficiently large to power a strong radio-jet according to the spin-paradigm ($L_1 \gg L_2$). Its upper limit is given by $M_1 c R_g = G M_1^2/c$, with R_g being the gravitational radius. For the orbital angular momentum we have $L_{\bullet\bullet} = M_1 \sqrt{G M_1 a}/\sqrt{q(1+q)}$, where $q = M_1/M_2 \geq 1$ is the mass-ratio of both BHs and a is the semi-major axis. Thus the ratio of these two angular momenta is

$$\frac{L_{\bullet\bullet}}{L_1} = \frac{1}{\sqrt{q(1+q)}} \sqrt{\frac{a}{R_g}}. \tag{19}$$

It is a very interesting question now, what actually dominates the final spin of the merged black hole, $L_\bullet$. When the distance

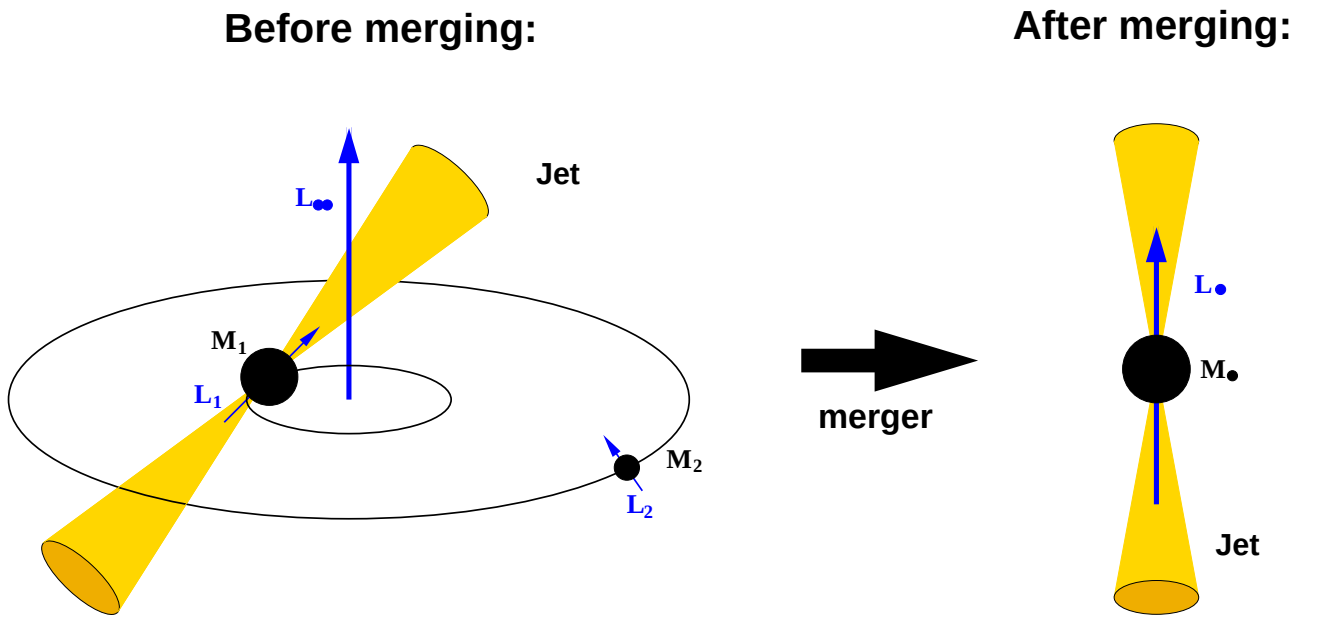

Fig. 9. This figure illustrates the change of the direction of the spin of the BH, induced by the merger of 2 massive BHs, and consequently the change of the direction of the jet. The left panel shows the situation before the merger, when the jet is aligned with the individual spin of the primary black hole of the binary system. The orbital angular momentum $L_{\bullet\bullet}$ of the BBH and the spins of both BHs (L_1 and L_2) are randomly orientated to each other, since no direction of the plane of the merging galaxies is preferred relative to the spin of both the BHs in their centers. After the BHs coalesced (right panel), the different spins combine to that of the merged BH with a new direction ($L_\bullet$). The jet emanating from the merged BH will be aligned with the new spin, which will be dominated by $L_{\bullet\bullet}$, and therefore has to jump from its orientation before the merger (L_1) into this new direction.

of both BHs has shrunk to about the last stable orbit ($R_{\rm ls} = 6\,R_{\rm g}$ in case of zero spin, and in case of a Kerr BH it depends on the inclination, see Chirvasa 2002) due to the emission of gravitational radiation, general relativistic effects become important. At this distance the orbital angular momentum dominates over the maximum possible spin of M_1, up to a mass-ratio of $q = 2$. This is actually a conservative limit since we neglected the last stable orbit around M_2. Hence the spin of the merged BH might be dominated by $L_{\bullet\bullet}$ rather than L_1, with the merged black hole $M_\bullet$ spinning close to its maximum value $L_\bullet = GM_\bullet^2/c$. This situation is shown in the right panel of Fig. 9. A new powerful radio-jet is emanating from the center, aligned with the BH's spin which is pointing in the direction of $L_{\bullet\bullet}$, and therefore parallel to the symmetry-axis of the torus. This means that the jet flips into a new direction. The angle enclosed by the old and new jet-axis corresponds to that between L_1 and $L_{\bullet\bullet}$ and hence can assume any value. After the merger the old jet is not fed anymore and its lobes will slowly fade away, while the new jet is digging its way through the ambient medium and the polar caps of the torus.

This might be the explanation for some of the most peculiar objects seen on the sky, the X-shaped radio-galaxies. They show a secondary, presently non-active pair of lobes, which is larger than and sometimes almost perpendicular to the presently active pair (Parma et al. 1985; Rottmann et al. 1998; Rottmann 2001), which we interpret in this picture as the new jet. This scenario is also in agreement with the involved time scales of some 10^7 yr for the merger and $\sim 6{\times}10^7$ yr in B2 0828+32 for the spectral aging of the secondary lobes (Rottmann 2001, priv. comm. H. Rottmann).

Such a major merger will also increase the accretion-rate onto the BH which might be in favour of the arguments of Meier (2001), who suggests an association of jet production with geometrically thick accretion flows and BH rotation.

For larger mass-ratios ($q > 2$) the possible influence of $L_{\bullet\bullet}$ on the final BH spin is decreasing, and therefore also the bending of the jet into a new direction will have a smaller amplitude. Thus we do not expect a jump of the jet in minor mergers where $M_2 \ll M_1$ and therefore $L_{\bullet\bullet} \ll L_1$ (see Eq. (19)) and ascribe the phenomenon of X-shaped radio-galaxies to recent major mergers, where one of the progenitors already had a powerful radio-jet. If radio strength is correlated with the spin of the BH, then the observations imply that a BH merger of spinning black holes leaves the ratio of spin to mass J/M large.

Before the two BHs finally coalesce, the surrounding patchy torus will have emerged on time scales of 10^7 yr (Paper I) in the plane of the merger, with its symmetry axis pointing along the binary's angular momentum. As long as the semimajor axis of the BBH is much larger than the last stable orbit of M_1, the old jet of the primary AGN is unaffected by M_2 and still fed, if the feeding mechanism from the accretion disk is not interrupted. Because the orientation of this jet is not correlated with that of the torus, it might flow into the solid angle covered by the torus, where it will interact with stellar winds and ISM in between. After the BHs coalesced the young past-merger jet is digging its way through the polar cap region of the torus, flowing along its symmetry axis. So both jets, the old and new, are interacting on sub-kpc scales with the ambient clumpy medium producing strong radio emission. This might be the cause of the so called Compact Symmetric

Objects (CSO), which is a class of powerful radio sources consisting of high unbeamed luminosity radio emission regions separated by less than 1 kpc and situated symmetrically about the center of activity (Phillips & Mutel 1982; Wilkinson et al. 1994). It is thought that the high-brightness regions are due to hot spots and mini-lobes, which are created by the termination of jets streaming out into opposite directions from the center, see Owsianik & Conway (1998) and references therein. Instantaneous speed variations of some components in CSO 0710+439 are most simply explained by interactions with a dense cloud medium, while other components are rapidly advancing through an intercloud medium. The expansion velocities are all of order $0.2\,h^{-1}c$ and therefore the age of these sources is estimated to be a few thousand years, showing that they are young rapidly growing sources (Owsianik et al. 1998; Owsianik et al. 1999). It is concluded that CSOs are probably young extragalactic radio-sources which will evolve via Medium-size Symmetric Objects into Large-size Symmetric Objects such as lower luminosity FR II double radio-sources (Fanti et al. 1995; Readhead et al. 1996; Owsianik & Conway 1998).

If the X-shaped radio galaxies are correctly explained with our proposed picture, the resulting gravitational wave pattern will strongly depend on the orientation of the three relevant spins (Chirvasa 2002) and therefore on the re-orientation of the primary black hole. It experiences a spin-flip in this picture.

6. A patchy torus–explanation for BAL QSOs and transition from type 1 to 2

The broad absorption line (BAL) quasars comprise about 10% of the optically selected quasars (i.e. Antonucci 2002b or Schmidt & Hines 1999), but since they are hard to find at optical wavelengths, their real fraction is thought to be in the range 20%–30%. Moreover the BAL covering factor is thought to be much less than unity and consequently there must be many objects, if not all, being intrinsically the same as BAL quasars, but not classified as such if seen from other directions. The region which is responsible for the formation of the BAL partially absorbs the broad emission lines, and therefore it must be outside the BLR. Also the polarization in the broad emission lines is observed to be lower than the polarization in the absorption troughs of the BALs.

Inside the torus, with its inner edge close to the evaporation radius of dust (∼1 pc) the heated matter will be accelerated and streams away from the nucleus through the gap between jet and torus either in form of clouds or as a wind. Here, above the surface where the density of the torus gradually decreases, the clouds are exposed to more intense radiation. These arguments fit well into the unification model, where the BAL QSOs are quasars seen at intermediate inclination angles, with the line of sight grazing the surface of the obscuring torus (Weymann et al. 1991; Voit et al. 1993) and thus is supported by our model.

With the assumption that the fraction of BAL QSOs of $\chi = 0.2$ to 0.3 represents the covering factor $C_{\rm BAL}$ in the same range (Weymann 1997), we can estimate the solid angle they comprise. We just have to solve the equation of the covering factors, $\chi = C_{\rm BAL}/C_{\rm QSO}$, for the polar angle $\theta_{\rm BAL}$, using the relations $C_{\rm QSO} = 1 - \cos\theta_{\rm trs}$ and $C_{\rm BAL} = \cos\theta_{\rm BAL} - \cos\theta_{\rm trs}$. In this notation the QSO exhibits BAL features if seen under inclination angles in the range $\theta_{\rm BAL} \lesssim \theta_{\rm incl} \lesssim \theta_{\rm trs}$. Assuming the half-opening angle of the torus to be $\theta_{\rm trs} = 45°$ and using the above fractions of BAL QSOs $\chi = 0.2$ and 0.3 we obtain $\theta_{\rm BAL} = 40°$ and 37° respectively. Hence for an intermediate inclination angle in the range of about

$$38° \lesssim \theta_{\rm incl} \lesssim 45°$$

the observed quasar will appear as a BAL QSO, in agreement with Schmidt & Hines (1999) who find BAL QSOs to be typically 2.4 times more polarized in the optical than QSOs.

Among the BAL QSOs the subclass of low-ionization absorbers shows evidence to be stronger polarized and to be reddened by dust (Sprayberry & Foltz 1992; Egami et al. 1996). Green et al. (2001) assumed that the same intrinsic power-law with index $\Gamma \approx 1.8$, which is consistent with the mean slope of radio quiet QSOs and has been derived for high-ionization BAL QSOs, applies to all BAL QSOs and is partially covered. This assumption has been confirmed in some recent publications (Gallagher et al. 2001; Green et al. (2001); Gallagher et al. 2002). For low-ionization BAL QSOs, which are weak in X-rays, Green et al. (2001) infer that they are enshrouded by an additional intrinsic column density of nearly $10^{23-24}\,{\rm cm}^{-2}$. These low-ionization BAL QSOs have been proposed by Brotherton et al. (1997) as the most edge-on QSOs.

For larger inclinations than the intermediate range the line of sight will intersect with more absorbing material since it approaches the surface of the patchy torus, which does not have a sharp defined edge. Consequently less of the BLR is seen directly and the fraction of scattered light as well as the polarization is increasing. With increasing inclination the view to the nucleus is increasingly blocked by the torus and the quasar will appear more reddened (IRAS QSO) till finally, if seen edge on, it will appear as a QSO of type 2 (ULIRG or FR II radio galaxy). On the other hand, objects seen at lower inclinations don't suffer absorption of the central radiation by the torus and are classified as quasars.

In the special case of the quasar FIRST J101614.3+520916 Gregg et al. (2000) find BAL features in the optical and radio loud emission from lobes of classic FR II type at the same time. According to the authors this quasar has some properties in common with low-ionization BAL QSOs, as for example higher reddening. They deduce an inclination of the jet-axis to the LOS of more than 40° and conclude that this quasar is in contradiction with the orientation model as explanation for BAL QSOs. Gregg et al. (2000) suggest that this quasar rather happens to be seen in a rare and short-lived state, showing both, BAL features and developed radio lobes at the same time, and postulate that it is a rejuvenated quasar, possibly through merger. Contrary to this conclusion we claim that these observations actually support the orientation model. According to the above numbers, BAL QSOs are seen at intermediate inclination angles in the range between ∼38° and ∼45°, in very good agreement with the inclination obtained for this quasar. Thus the LOS to the core of J101614.3+520916 is grazing the surface of the patchy torus, whose constituting absorbers,

the stellar winds, are increasing in number density towards the equatorial plane. At higher inclinations the torus would block the free view to the center completely and no BALs could be detected, so that this object would appear as a typical FR II quasar. This is also in agreement with BAL QSOs, that show large radio lobes, being so rare. We do not exclude evolutionary effects, but as shown above, we also expect a merger to seriously affect the jet, what should be detectable. And the question to be answered for the evolutionary/rejuvenated scenario is: What is the explanation then for the difference between the radio-quiet BAL and non-BAL quasars?

Due to the patchy nature of the torus, we propose partial covering absorption plus scattering in order to fit the spectra of BAL QSOs. Another important consequence of the patchy torus is, when the absorbing clouds are moving through the line of sight, the column density changes and variations in the spectrum are expected. This is then a natural explanation for the variability of the BAL quasar PG 2112+059 between the *ROSAT* and *ASCA* observations on scales of 6 yr, being due to changes in the absorber, either the ionization parameter, or the column density. We investigate such variabilities in more detail in the following.

One observable consequence of an obscuring patchy torus, as developed in this paper, is a possible variation of the absorption properties, i.e. the column density. A covering factor of the torus of about unity means that not necessarily all lines of sight through the torus to the central radiation source are covered and that due to the motions of the stars in the torus under the influence of the central BHs such gaps will form and will be closed continuously.

When an obscuring cloud or stellar wind of the torus is moving into (out of) the line of sight of the observer to the radiation source, the column density will drastically increase (decrease) and the source will gradually appear much weaker (brighter) in luminosity. For our chosen AGN with $M_1 = 10^8\,M_\odot$ we obtained the circumnuclear torus to be located in a distance of a few parsecs to the center. The radius of the wind of the obscuring stars we computed to be of order of 0.002 pc. For a star moving on Keplerian orbits in the potential of such a BH, the velocity is $v = \sqrt{GM_1/r}$. Therefore the time required for the star's wind to move along its diameter from one edge to the other through the line of sight is

$$t_{\rm var} = 2\frac{R_{\rm w}}{v} \approx 10\,\frac{R_{\rm w}}{0.002\,{\rm pc}}\left(\frac{r}{3{\rm pc}}\right)^{\frac{1}{2}}\left(\frac{M_1}{10^8\,M_\odot}\right)^{-\frac{1}{2}}\,{\rm yr}\,. \qquad (20)$$

Consequently variations of the column density and the luminosity are expected to happen on scales of a decade. Since the density of stars is enhanced towards the equatorial plane of the torus it is likely that there is more than one star in the line of sight and thus a transition from optically thick to thin or vice versa will be a rare event in an edge-on seen torus. But if the LOS grazes the surface of the torus the chance to observe such a transition will be higher. And indeed there are a couple of observations which fit well to this interpretation. Before comparing the above computed time scale for a transformation from type 1 → 2 with observations, we want to scale it just in a simple way with the mass of the central BH.

Assuming the luminosity to be proportional to the eddington, $L_{\rm edd} = 4\pi GcM_1 m_{\rm p}/\sigma_{\rm Th}$, we have $L \propto M_1$. Thus with Eq. (9) the wind radius scales as

$$R_{\rm w} \propto \frac{r^2}{L} \propto \frac{r^2}{M_1}.$$

Together with $v_{\rm kep} \propto \sqrt{M_1/r}$ the dependency of the time on mass and radius is:

$$t_{\rm var} \propto \frac{r^{5/2}}{M_1^{3/2}}.$$

There are now at least two possibilities for the choice of the inner radius of the torus:

(1) The evaporation radius, for which we have $r_{\rm evap} \propto L^{1/2} \propto M_1^{1/2}$ (see Eq. (7)). Thus we obtain the dependency

$$t_{\rm var} \propto M_1^{-1/4}\,, \qquad (21)$$

what means that the time required for a cloud passing through the line of sight is decreasing with increasing mass of the central BH.

(2) Another choice for the radius of the torus is the distance of the BHs, when the binary is hard, since the simulation showed that this coincides to within a factor of a few with the radius of the torus (Paper I). According to Milosavljević & Merritt (2001) the binary becomes hard at a semi-major axis $a_h = GM_\bullet/8\sigma^2$. Using the relation

$$M_\bullet = 1.3\times10^8\,M_\odot\left(\frac{\sigma}{200\,{\rm km\,s^{-1}}}\right)^{\alpha}\,,$$

with $\alpha = 4.72(\pm0.36)$ (found by Meritt & Ferrarese 2001a, 2001b) we get

$$t_{\rm var} \propto M_1^{(\alpha-5)/\alpha} \approx M_1^{-8/135}\,. \qquad (22)$$

Again there is a negative exponent, albeit small, so that t is decreasing with increasing M_1, as for $r = r_{\rm evap}$.

Since the exponents in the time-mass relation are much smaller than 1 for both choices of the inner radius of the torus, the transition-time does not depend strongly on the mass of the central BH, and is almost constant on orders of 10 yr. For a patchy absorber it is possible that more than one cloud or stellar wind happens to block the line of sight, and depending on their individual velocities and directions in which they move, it is possible that the decrease and increase of the central flux proceeds on different time scales.

In the following we will give some examples of sources which are in agreement with our patchy torus model within the unification scheme and show the expected variations in column density on scales of a decade.

NGC 7582: compared to the *EXOSAT* observations in 1983 Warwick et al. (1993) detect 4 yr later with *Ginga* a significant increase of the column density to $\sim4.6\times10^{23}\,{\rm cm^{-2}}$ by a factor of about 3. While the spectral index between the two *ASCA* observations from November 1994 and 1996 does not show a significant variation the column density seems to have increased by ∼44% (Xue et al. 1998). In the hard and soft X-ray band of the *BeppoSAX* observation in November 1998 Turner et al. (2000) find the nucleus clearly to have brightened since

the 1994 *ASCA* observation. While this increase seems to be consistent with the appearance of holes in the full screen ($1.4 \times 10^{23}\,\mathrm{cm}^{-2}$) the authors also find evidence for larger absorption at the *BeppoSAX* epoch with a "thick absorber" covering 60% of the nucleus, corresponding to a half-opening angle of a torus of ∼53°, which has a column density of $1.6 \times 10^{24}\,\mathrm{cm}^{-2}$. Both these values are in good agreement with the column density we computed for the torus and that what is obtained if the matter would be smoothly distributed in the volume of the torus (see Eq. (23) in Sect. 7). The total timescale of about 15 yr for major variations in the column density is in very good agreement with our predictions.

NGC 2992: this source has been monitored over a time of 20 yr with different telescopes (*HEAO*: Mushotzky 1982; Singh et al. 1985; *Einstein*: Halpern 1982; Turner et al. 1991; *EXOSAT*; Turner & Pounds 1989; *Ginga*: Nandra & Pounds 1994; *ASCA*: Weaver et al. 1996 and *BeppoSAX*: Gilli et al. 2000). During 16 yr the 2–10 keV flux declines steadily by a factor of 20 and is 4 yr later back to its initial value measured in 1978. Over this time range the spectrum retains a constant shape, which is only different in the low state observed by *ASCA* in 1994, when there are also no short-time variabilities are seen. This is actually what is expected, since according to our idea in this stage the direct view to the center is blocked by a cloud.

NGC 4051: while the flux in the range 2–10 keV of this Seyfert 1 galaxy has been almost constant for more than 10 yr till the *RXTE* observations by Uttley et al. (1998) it is measured to be 20 times fainter 1.5 yr later with *BeppoSAX* in 1998 by Guainazzi et al. (1998). The time scale of ∼1.5 yr for the decrease of the luminosity by a factor of 20 might be too short to be accounted for by a cloud of the patchy torus moving into the line of sight.

NGC 1365: between the *ASCA* observations and the *BeppoSAX* in August 1997 three years later the flux in the range 2–10 keV has increased by a factor of 6 (Risaliti et al. 2000).

NGC 3227: in their comparision of the data from *ASCA* observations in 1993 and 1995 and *ROSAT* observations in 1993 George et al. (1998) show that the column density of the ionized absorber increased by about an order of magnitude, i.e. from $N_\mathrm{H} \sim 3 \times 10^{21}\,\mathrm{cm}^{-2}$ in 1993 to $N_\mathrm{H} \sim 3 \times 10^{22}\,\mathrm{cm}^{-2}$ in 1995. They think this to be most naturally explained by a cloud of material moving into the cylinder of sight.

7. Influence and implications of the binary's mass-ratio

Our simulations in Paper I showed that for a decreasing mass-ratio of the BHs ($q = M_1/M_2 \geq 1$, with $M_1 = 10^8\,M_\odot = \mathrm{const.}$) the fraction of the ejected stars is increasing. But to extract the bigger amount of angular momentum from a more massive binary ($L_{\bullet\bullet} = \sqrt{GM_1^3 a}/\sqrt{q(q+1)}$), the increased fraction of ejected stars is not sufficient, so that the star cluster has to be more massive in order to absorb the binary's angular momentum and to enable the BHs to coalesce. Therefore the amount of bound stars has to increase with the mass M_2 of the secondary BH, and so the torus becomes more massive.

As we have pointed out in the discussion of the influence of the mass-ratio, the inner regions become increasingly unstable for more massive secondary BHs, so that at the inner edge of the torus the stars are moving on almost circular orbits to avoid violent interactions with the binary. For sufficiently small mass-ratios a more sharp defined torus forms during the late stages of the merger, while for young mergers and mergers with large mass-ratios a more diffuse and shell-like density distribution of the stars is maintained. This is clearly visible in Figs. 2 and 14 of Paper I, which also show a larger half-opening angle of the torus in the range 50° to 60° for $q = 1$ (i.e. $M_2 = M_1$) compared to about 45° for $q = 10$. This is due to the stronger torque that is exerted by the binary with smaller q on stars in the polar cap region, and therefore less orbits are passing through this region.

In major mergers we also expect the accretion rate on the central BH to be much higher and thus these mergers to be much more luminous than minor ones. This is in agreement with the idea that the opening angle depends on the luminosity, being larger for the more luminous AGN. Consequently the radiation pressure acting on the torus and its stars is less in minor mergers, and according to Eq. (9) the radius of the stellar winds can extend to much larger radii, not being stretched into elongated tails. Hence the column density along the LOS to the center is diminished and the torus becomes optically thin (see also Sect. 4).

This can be illustrated with a simple order-of-magnitude estimate. The volume of the torus with half-opening angle θ_trs within the radial limits r_in and r_out is $V_\mathrm{trs} = \frac{4\pi}{3}(r_\mathrm{out}^3 - r_\mathrm{in}^3)\cos\theta_\mathrm{trs}$. If we distribute the total mass contained in the stellar winds homogeneously in this volume, the number density of hydrogene is

$$n_\mathrm{H} = \frac{M_\mathrm{d,total}}{1.4 Z_\mathrm{d} m_\mathrm{p} V_\mathrm{trs}}.$$

Integrating along the line of sight from r_in to r_out, yields for the column density of such a homogeneous torus

$$N_\mathrm{H} = \frac{3\,M_\mathrm{d,total}}{5.6\,\pi Z_\mathrm{d} m_\mathrm{p} \cos\theta_\mathrm{trs}} \frac{r_\mathrm{out} - r_\mathrm{in}}{r_\mathrm{out}^3 - r_\mathrm{in}^3} = 4.8 \times 10^{23}\,\mathrm{cm}^{-2}. \qquad (23)$$

The total dust mass of the torus is $350\,M_\odot$ (see Eq. (18)) and for the geometry of the torus we used the same values as in Sect. 4, i.e. 60° for the half-opening angle and 1 and 5 pc for the inner and outer radius respectively. This gives less than half the column density of the patchy torus in Sect. 4, when the radiation pressure is strong enough to turn back the wind into elongated tails. Thus a torus with smoothly distributed matter would be optically thin, showing that a sufficiently high luminosity is necessary in order to maintain an opaque torus. According to our results from Paper I the optical thickness of tori as products from major mergers ($M_1 = M_2 = 10^8\,M_\odot$) compared to minor mergers ($M_1 = 10^8\,M_\odot$, $M_2 = 10^7$ or $10^6\,M_\odot$) is further enhanced due to the higher absolute amount of stars that stay bound in the potential of the binary, even though a larger fraction is ejected. This is plausible, since in a minor merger a less massive stellar cluster is surrounding the secondary BH, which is dragged to the common center by dynamical friction.

Thus we come to the following conclusion: in a major merger with two BHs of comparable mass (∼$10^8\,M_\odot$) more

stars are brought to the common center and stay bound in the potential of the binary, where they enhance the optical thickness of the torus they constitute. Because of the stronger torque exerted by the BHs, the half-opening angle of this torus is larger than in a minor merger. Since the accretion rate is expected to be close to the Eddington limit, the stellar winds are exposed to strong radiation pressure from the center, which shapes the winds into elongated cometary tails, pointing radially away from the center. Hence they are sufficiently opaque as to make the stellar torus optically thick. With increasing time the accretion rate and consequently the luminosity will decrease, so that the stellar winds in the torus will become less collimated. Therefore the opacity of the torus will decrease also as an evolutionary effect of the AGN.

If, on the other hand, a $10^8\,M_\odot$ BH merges with a black hole of much lower mass, fewer stars are involved and the torus will contain less stars. Because of the smaller torque of the binary, the torus is more diffuse and the opening angle is smaller. According to our simulation, such a torus looks like that of a major merger in early stages (compare the Figs. 2 and 14 in Paper I). In a minor merger also the accretion rate will be smaller and consequently the luminosity. This results in less radiation pressure acting on the stellar winds, which are not shaped into elongated tails, and thus the opacity of the torus, containing already fewer stars, is even more diminished.

This seems to be in agreement with the observations: Major mergers of galaxies of comparable size with BHs in their centers of comparable mass will violently stir up the stars, gas and dust, and finally assume an elliptical rather than a spiral shape. According to our finding above, ellipticals then should harbour AGN with tori having larger half-opening angles than spirals and thus on average type 1 nuclei should be detected more often in elliptical than spiral hosts. This is supported by the survey of Malkan et al. (1998), who find Seyfert 1 nuclei to reside on average in more early type hosts than Seyfert 2 nuclei.

It has been emphasized (i.e. Antonucci 2002a and references therein) that there must be a range of covering factors for dusty tori, with the type 2-classified objects having higher average covering factors. It is concluded that the populations are therefore intrinsically different in their statistical properties to some extend. Maybe the mass-ratio of the BHs and the evolution of AGN are the reasons for statistically different covering factors.

If the nucleus happens to be oriented to us in a way that the line of sight grazes the edge of the torus, the probability to see the nucleus still directly through a gap in the edge of the clumpy structure is more probable for large than small mass-ratios. This might be an explanation for NGC 4151, which is a type 1 and has an aligned NLR too. But HST images show a cone on subarcsec scales (Antonucci 1993). According to the strict unified model this is not expected since a type 1 should only be seen if the observer is inside the unobscured solid angle so that a projected ionization cone can not be seen. In our model the patchy torus can have gaps or holes, the more likely the larger q is and the closer the line of sight comes to the edge of the torus which is not clearly defined. In the case of NGC 4151 the observer seems to be outside the opening angle. But through a gap in the torus close to its edge enough radiation can escape and is seen directly so that NGC 4151 is classified as a type 1.

M 87, the nearest giant elliptical galaxy ($z = 0.0043$), has been observed at $10.8\,\mu$m wavelength by Perlman et al. (2001). If there is a dusty opaque torus it should be visible in the reradiated IR, but the authors find only little evidence of thermal emission from dust. Because of its large BH mass ($\sim 3\times10^9\,M_\odot$, Marconi et al. 1997) and the giant elliptical shape it is likely to have undergone a major merger in the past. Since then the fuelling of the AGN probably has decreased and the luminosity dropped to its current estimated value of 10^{42} erg/s (Whysong & Antonucci 2001), what fits to M 87 being on the FR I-II border, as well in morphology as in radio power (Owen et al. 2000). This luminosity is too weak as to maintain an opaque torus, which also might have been dissolved since the merger (see Sect. 4.2, lifetime of the torus). A possible minor merger afterwards most likely would not have sufficiently increased the luminosity and replenished the torus with stars in order to form a dusty and opaque torus again. Whysong & Antonucci (2001) measured the reradiation from nuclear hot and warm dust, which must be emitted according to the unification scheme by the torus that absorbs the radiation from the AGN it surrounds. This radiation should be found in almost any hidden AGN and provides an estimate of the unblocked central luminosity. While for Cyg A at redshift 0.057 (more than 10 times the redshift of M 87), with an estimated luminosity $\sim 1.5\times10^{45}$ erg/s, they could detect this component, it is much weaker in M 87, where no hidden nucleus can be found. The estimated mass accretion in Eddington units $\dot{M}/\dot{M}_{\rm edd}$ is in the range $10^{-3.5}$ to 10^{-3}, which is much less than 1/50 (Liu et al. 1999). Below this value a thin Shakura-Sunyaev disk can not survive (Meyer et al. 2000). With respect to its large mass, M 87 seems to host a starving black hole in the center.

This is in line with the results of Meisenheimer et al. (2001), who compared galaxy-quasar pairs from the 3CR catalogue in the IR range from 5 to $180\,\mu$m to test the unification scheme for luminous radio galaxies and quasars. The pairs have been selected such that they match in 178 MHz luminosity, which is thought to be emitted fairly isotropic, and redshift in order to minimize the effects of cosmic evolution. They can not distinguish the pairs by their mid- and far-infrared properties, what strongly supports the unification scheme. The authors also find the ratio of thermal dust power νF_ν, averaged over 60 and $100\,\mu$m, to the radio power at 178 MHz to correlate better with redshift than with luminosity. They suggest that this might be due to the thermal power of a radio source being primarily controlled by the accretion rate, with sources accreting at high rates being more numerous at large redshifts, when major mergers have been more frequently than today.

8. Summary and conclusions

In Paper I we showed that a central geometrically thick torus, comprised of stars, results at a distance of order 3 pc from the center as a product from the merger of two galaxies and their central supermassive black holes. This stellar torus has to be about as massive as the binary black hole in order to enable

the BHs to get rid of their orbital angular momentum and to coalesce on scales of 10^7 yr.

In the present article we proved that this torus with its patchy structure is in very good agreement with the properties of the ubiquitous torus in AGN, as are demanded in the unification scheme and deduced from observations. About 1% of these stars have strong enough winds in order to obscure the central radiation source for lines of sight passing through their winds. The central radiation pressure shapes the winds of these obscuring stars in the torus into elongated tails, pointing radially away from the central source. Consequently their azimuthal extension is about 4×10^{-3} pc, such that these winds along their tails are optically thick, and that their total covering factor within the torus amounts to ∼1. Thus these winds cause the geometrically thick torus also to be optically thick with column densities of about $10^{24}\,\mathrm{cm}^{-2}$, just as is observed. Also the inner radius of about 1 pc coincides with the evaporation radius of graphite dust grains (Lawrence 1991), what has been previously assumed to be the inner edge, and what is also the distance where the BHs become hard (Milosavljević & Merritt 2001) and which defined the inner edge in the simulation of Paper I.

In Sect. 5 we demonstrated that the recent merging of two comparable supermassive BHs, the prerequisite for the forming of the opaque torus, can explain the X-shaped radio galaxies. According to the spin-paradigm, fast spinning BHs are powering strong radio jets in radio galaxies. If such a galaxy merges with another one hosting a BH of comparable mass, the orbital angular momentum of the resulting BBH dominates over the maximum possible spin of the primary BH, at least till their major axis has shrunk to the last stable orbit. When the BHs eventually merge, the final spin might be dominated by the orbital angular momentum, leaving the merged BH spinning close to its maximum value. As a consequence a new powerful jet emanates into the direction of the orbital angular momentum, which is aligned with the symmetry axis of the torus. Therefore this jet streams through the ambient medium, producing strong radio emission, while the old jet's lobes, not fed anymore, are slowly fading away. The time scales of spectral aging of these lobes is close to the merger-time of the BHs and thus supports further this interpretation. The old jet might intersect with the torus and consequently would interact with its clumpy medium, also resulting in strong radio emission. This could be an explanation for the Compact Symmetric Objects, which are thought to be young and probably evolve into large-size Symmetric Objects, such as lower luminosity FR II double radio sources.

With such a patchy torus-model, the BAL QSOs fit well into the sequence in which a QSO appears as Blazar if seen pole-on. As the inclination angle increases it appears as a normal quasar, then high ionization BAL QSO, low ionization BAL QSO and finally, when the line of sight lies in the equatorial plane of the torus, as ULIRG. For the intermediate agles the line of sight grazes the surface of the torus, explaining the features of the BAL QSOs. In the sample studied by Gallagher et al. (2002), for most of them a partial-covering absorber provides a significantly better fit than other models, confirming our torus model. The detected variability of the BAL quasar PG 2112+059 on scales of 6 yr is ascribed to changes in the absorber, probably the column density. This is just the time the stellar winds in the torus need to move through the line of sight. In Sect. 6 we give more examples of objects whose column densities are observed to change considerably on these time scales. They are very strongly supporting the idea of the patchy torus, since the winds of the stars, moving in the potential of the central BH, have the right size and optical depth at the appropriate distance to the center to yield such strong variations in N_H on the right time scales, as they move through the line of sight. Due to the stellar motion gaps in the torus will be continuously opened and closed.

For major mergers the resulting torus is more massive and therefore has a larger column density (see Sect. 7). Because the accretion-rate and consequently the luminosity will be higher than in minor mergers, the radiation pressure acting on the winds is stronger, being able to bend the winds into elongated tails. This further increases the torus' opacity compared to that of minor mergers. Since the torque of a more massive binary acting on the stars is stronger, the opening angle of the resulting torus is wider and therefore correlates with the central luminosity, as has been suggested in the past. But the column density of the torus will also change with time, as the luminosity decreases when the accretion rate weakens. Thus the opacity depends on the mass-ratio of the merging black holes and on evolutionary effects of the AGN. Hence we expect to observe type 1 AGN more likely in elliptical host galaxies at larger redshifts, where major mergers occured more frequently. We also expect higher covering factors of type 2 objects. In their survey of Seyfert galaxies Malkan et al. (1998) find on average type 1 AGN to be hosted by more early type galaxies than Seyfert 2s, in agreement with our reasoning.

Previous compact torus models with a smooth distribution of the matter all faced the same problem in predicting a too narrow infrared spectrum, and to fit the data, additional NIR sources had to be invoked (Pier & Krolik 1993; Granato & Danese 1994; Efstathiou & Rowan-Robinson 1995; Alonso-Herrero et al. 2001). As has been already mentioned in these papers, it is obvious that a patchy torus will tend to increase the dust temperature in the outer parts, since they are exposed to the radiation from the center shining through gaps in the inner parts of the torus. This will tend to broaden the IR spectrum. Such models also exhibit strong emission or absorption 9.7 μm silicate features, which are usually not in agreement with the observations. Another problem is to achieve the geometrical thickness of the torus, which according to Pier & Krolik (1992b) can be supported by radiation pressure. But for a low luminosity source they need the torus to be clumpy and introduce a radiation pressure driven random motion of the clumps in order to maintain the thickness of the torus.

In the model we proposed here and in Paper I, the torus is naturally thick as a result of the stars moving in the potential of the binary. The patchy structure inevitably leads to self-shielding of the stellar winds and also within the winds. This probably has an effect on the temperature of the gas and dust as a function of the distance to the central source. Both, the selfshielding and the temperature distribution in the torus will have a strong influence on the reprocessed and reemitted

radiation. The calculation of the temperature distribution and spectra of the winds and the torus they constitute would involve a full threedimensional treatment, so that radiation-transfer calculations are well beyond the scope of this paper and we can not give a comment on possible silicate features as function of the inclination angle.

The torus model proposed in these two articles gives a coherent picture with respect to the formation of the torus, its evolution and application to observations in terms of the unification scheme.

Acknowledgements. This article as well as Paper I are based on on the first author's Ph.D. thesis from june 2000 (Zier 2000). CZ would like to thank R. R. J. Antonucci, M. Malkan, D. Merritt, G. Smith, and S. Westerhoff for their helpful discussions and their generous and kind hospitality (fall 2000). CZ also acknowledges the longterm support by the MPIfR. PLB would like to thank Drs. A. Donea and R. Protheroe for extended discussion on tori, and their hospitality at Adelaide. PLB also acknowledges the discussions with R. R. J. Antonucci, M. Malkan, G. Schäfer and N. Straumann. PLB and CZ also like to especially thank M. Chirvasa for the discussions on her work of gravitational radiation of a black hole binary, her Ph.D. thesis at the University of Bukarest of February 2000 (Chirvasa 2002). High energy physics in PLB's group is supported by AUGER-Theory grant 05 CU1ERA/3 from DESY/BMBF.

References

Alexander, T., & Netzer, H. 1994, MNRAS, 270, 781
Alexander, T., & Netzer, H. 1997, MNRAS, 284, 967
Alonso-Herrero, A., Quillen, A. C., Simpson, C., Efstathiou, A., & Ward, M. J. 2001, AJ, 121, 1369
Antonucci, R. 1993, ARA&A, 31, 473
Antonucci, R. R. J. 2002a, in Proc. of the IAU Colloq. 184, AGN surveys, Byurakan, Armenia, June 2001, ASP Conf. Ser., in press [astro-ph/0110343]
Antonucci, R. R. J. 2002b, Astophysical Spectropolarimetry, 151 [astro-ph/0103048]
Antonucci, R. R. J., & Miller, J. S. 1985, ApJ, 297, 621
Baribaud, T., Alloin, D., Glass, I., & Pelat, D. 1992, A&A, 256, 375
Barthel, P. D. 1989, ApJ, 336, 606
Barvainis, R. 1987, ApJ, 320, 537
Biermann, P., & Harwit, M. 1980, ApJ, 241, L105
Biermann, P., & Shapiro, S. L. 1979, ApJ, 230, L33
Biermann, P. L. 1989, in C, Mathematical and physical sciences, Cosmic Gamma Rays, Neutrinos, and Related Astrophysics, NATO ASI series. Ser., 270, 21
Boller, T., Fabian, A. C., Sunyaev, R., et al. 2002, MNRAS, 329, L1
Brotherton, M. S., Tran, H. D., van Breugel, W., Dey, A., & Antonucci, R. 1997, ApJ, 487, L113
Chini, R., Kreysa, E., & Biermann, P. L. 1989, A&A, 219, 87
Chirvasa, M. 2002, M.Sc. Thesis, University of Bukarest
Clavel, J., Wamsteker, W., & Glass, I. S. 1989, ApJ, 337, 236
Conway, J. E., & Blanco, P. R. 1995, ApJ, 449, L131
Edwards, A. C. 1980, MNRAS, 190, 757
Efstathiou, A., & Rowan-Robinson, M. 1995, MNRAS, 273, 649
Egami, E., Iwamuro, F., Maihara, T., Oya, S., & Cowie, L. L. 1996, AJ, 112, 73
Fanti, C., Fanti, R., Dallacasa, D., et al. 1995, A&A, 302, 317
Farouki, R. T., & Shapiro, S. L. 1982, ApJ, 259, 103
Gallagher, S. C., Brandt, W. N., Chartas, G., & Garmire, G. P. 2002, ApJ, 567, 37
Gallagher, S. C., Brandt, W. N., Laor, A., et al. 2001, ApJ, 546, 795
George, I. M., Mushotzky, R., Turner, T. J., et al. 1998, ApJ, 509, 146
Gilli, R., Maiolino, R., Marconi, A., et al. 2000, A&A, 355, 485
Granato, G. L., & Danese, L. 1994, MNRAS, 268, 235
Green, P. J., Aldcroft, T. L., Mathur, S., Wilkes, B. J., & Elvis, M. 2001, ApJ, 558, 109
Gregg, M. D., Becker, R. H., Brotherton, M. S., et al. 2000, ApJ, 544, 142
Guainazzi, M., Nicastro, F., Fiore, F., et al. 1998, MNRAS, 301, L1
Haas, M., Müller, S. A. H., Chini, R., et al. 2000, A&A, 354, 453
Halpern, J. P. 1982, Ph.D. Thesis, 4
Hoefner, S., Fleischer, A. J., Gauger, A., et al. 1996, A&A, 314, 204
Huchra, J., & Burg, R. 1992, ApJ, 393, 90
Kinney, A. L., Antonucci, R. R. J., Ward, M. J., Wilson, A. S., & Whittle, M. 1991, ApJ, 377, 100
Knapp, G. R., & Morris, M. 1985, ApJ, 292, 640
Krichbaum, T. P., Alef, W., Witzel, A., et al. 1998, A&A, 329, 873
Krolik, J. H., & Begelman, M. C. 1988, ApJ, 329, 702
Lawrence, A. 1991, MNRAS, 252, 586
Lawrence, A., & Elvis, M. 1982, ApJ, 256, 410
Liu, B. F., Yuan, W., Meyer, F., Meyer-Hofmeister, E., & Xie, G. Z. 1999, ApJ, 527, L17
Longair, M. S. 1981, High energy astrophysics (Cambridge: University Press)
Lovelace, R. V. E., Romanova, M. M., & Biermann, P. L. 1998, A&A, 338, 856
Macchetto, F., Capetti, A., Sparks, W. B., Axon, D. J., & Boksenberg, A. 1994, ApJ, 435, L15
MacDonald, J., Stanev, T., & Biermann, P. L. 1991, ApJ, 378, 30
Maiolino, R., Salvati, M., Bassani, L., et al. 1998, A&A, 338, 781
Malkan, M. A., Gorjian, V., & Tam, R. 1998, ApJS, 117, 25
Marconi, A., Axon, D. J., Macchetto, F. D., et al. 1997, MNRAS, 289, L21
Mathis, J. S., Rumpl, W., & Nordsieck, K. H. 1977, ApJ, 217, 425
Meier, D. L. 2001, ApJ, 548, L9
Meisenheimer, K., Haas, M., Müller, S. A. H., et al. 2001, A&A, 372, 719
Merritt, D., & Ferrarese, L. 2001a, MNRAS, 320, L30
Merritt, D., & Ferrarese, L. 2001b, ApJ, 547, 140
Meyer, F., Liu, B. F., & Meyer-Hofmeister, E. 2000, A&A, 354, L67
Miller, J. S., Goodrich, R. W., & Mathews, W. G. 1991, ApJ, 378, 47
Milosavljević, M., & Merritt, D. 2001, ApJ, 563, 34
Mulchaey, J. S., Mushotzky, R. F., & Weaver, K. A. 1992, ApJ, 390, L69
Mushotzky, R. F. 1982, ApJ, 256, 92
Nagar, N. M., & Wilson, A. S. 1999, ApJ, 516, 97
Nandra, K., & Pounds, K. A. 1994, MNRAS, 268, 405
Niemeyer, M., & Biermann, P. L. 1993, A&A, 279, 393
Oliva, E., Origlia, L., Kotilainen, J. K., & Moorwood, A. F. M. 1995, A&A, 301, 55
Osterbrock, D. E., & Shaw, R. A. 1988, ApJ, 327, 89
Owen, F. N., Eilek, J. A., & Kassim, N. E. 2000, ApJ, 543, 611
Owsianik, I., & Conway, J. E. 1998, A&A, 337, 69
Owsianik, I., Conway, J. E., & Polatidis, A. G. 1998, A&A, 336, L37
Owsianik, I., Conway, J. E., & Polatidis, A. G. 1999, New Astron. Rev. 43, 669
Pérez, E., Márquez, I., Marrero, I., et al. 2000, A&A, 353, 893
Parma, P., Ekers, R. D., & Fanti, R. 1985, A&AS, 59, 511
Perlman, E. S., Sparks, W. B., Radomski, J., et al. 2001, ApJ, 561, L51
Peterson, B. M. 1993, PASP, 105, 247
Phillips, R. B., & Mutel, R. L. 1982, A&A, 106, 21
Pier, E. A., & Krolik, J. H. 1992a, ApJ, 401, 99
Pier, E. A., & Krolik, J. H. 1992b, ApJ, 399, L23

Pier, E. A., & Krolik, J. H. 1993, ApJ, 418, 673
Pogge, R. W. 1989, ApJ, 345, 730
Readhead, A. C. S., Taylor, G. B., Pearson, T. J., & Wilkinson, P. N. 1996, ApJ, 460, 634
Risaliti, G., Maiolino, R., & Bassani, L. 2000, A&A, 356, 33
Rottmann, H. 2001, Ph.D. Thesis, University of Bonn
Rottmann, H., Dennet-Thorpe, J., & Klein, U. 1998, Astronomische Gesellschaft Meeting Abstracts, Abstracts of Contributed Talks and Posters presented at the Annual Scientific Meeting of the Astronomische Gesellschaft at Heidelberg, September 14–19, 1998, poster #P77, 14, 77
Rybicki, G. B., & Lightman, A. P. 1979, Radiative Processes in Astrophysics (John Wiley & Sons)
Sanders, D. B., Phinney, E. S., Neugebauer, G., Soifer, B. T., & Matthews, K. 1989, ApJ, 347, 29
Schmidt, G. D., & Hines, D. C. 1999, ApJ, 512, 125
Shull, J. M. 1983, ApJ, 264, 446
Singh, K. P., Garmire, G. P., & Nousek, J. 1985, ApJ, 297, 633
Sitko, M. 1991, in Variability of Active Galactic Nuclei, ed. H. R. Miller, & P. J. Wiita (Cambridge University Press), 104
Sprayberry, D., & Foltz, C. B. 1992, ApJ, 390, 39
Stecker, F. W., Done, C., Salamon, M. H., & Sommers, P. 1991, Phys. Rev. Lett., 66, 2697
Taniguchi, Y., & Anabuki, N. 1999, ApJ, 521, L103
Tinsley, B. M., & Larson, R. B. ed., 1977, The Evolution of galaxies and stellar populations
Tout, C. A., Eggleton, P. P., Fabian, A. C., & Pringle, J. E. 1989, MNRAS, 238, 427
Turner, T. J., Perola, G. C., Fiore, F., et al. 2000, ApJ, 531, 245
Turner, T. J., & Pounds, K. A. 1989, MNRAS, 240, 833
Turner, T. J., Weaver, K. A., Mushotzky, R. F., Holt, S. S., & Madejski, G. M. 1991, ApJ, 381, 85
Ueno, S., Koyama, K., Nishida, M., Yamauchi, S., & Ward, M. J. 1994, ApJ, 431, L1
Urry, C. M., & Padovani, P. 1995, PASP, 107, 803
Uttley, P., McHardy, I. M., Papadakis, I. E., Cagnoni, I., & Fruscione, A. 1998, in The Active X-ray Sky: Results from BeppoSAX and RXTE, Proc. of the Active X-ray Sky Symp., October 21–24, 1997, Rome, Italy, ed. L. Scarsi, H. Bradt, P. Giommi, & F. Fiore (Amsterdam: Elsevier, 1998), Reprinted from: Nuclear Physics B, (Proc. Suppl.), vol. 69/1-3. ISBN: 0444829903., 490
Voit, G. M., & Shull, J. M. 1988, ApJ, 331, 197
Voit, G. M., Weymann, R. J., & Korista, K. T. 1993, ApJ, 413, 95
Warwick, R. S., Sembay, S., Yaqoob, T., et al. 1993, MNRAS, 265, 412
Weaver, K. A., Nousek, J., Yaqoob, T., et al. 1996, ApJ, 458, 160
Weymann, R. 1997, in Mass Ejection from Active Galactic Nuclei, ASP Conf. Ser., 128, 3
Weymann, R. J., Morris, S. L., Foltz, C. B., & Hewett, P. C. 1991, ApJ, 373, 23
Whysong, D., & Antonucci, R. R. J. 2001 [astro-ph/0106381]
Wilkinson, P. N., Polatidis, A. G., Readhead, A. C. S., Xu, W., & Pearson, T. J. 1994, ApJ, 432, L87
Willott, C. J., Rawlings, S., & Blundell, K. M. 1999, in Quasars and Cosmology, ASP Conf. Ser., 162, 135
Wills, B. J. 1999, in Quasars and Cosmology, ASP Conf. Ser., 162, 101
Wilson, A. S., Braatz, J. A., Heckman, T. M., Krolik, J. H., & Miley, G. K. 1993, ApJ, 419, L61
Wilson, A. S., & Colbert, E. J. M. 1995, ApJ, 438, 62
Wilson, A. S., & Tsvetanov, Z. I. 1994, AJ, 107, 1227
Winters, J. M., Dominik, C., & Sedlmayr, E. 1994, A&A, 288, 255
Xue, S., Otani, C., Mihara, T., Cappi, M., & Matsuoka, M. 1998, PASJ, 50, 519
Young, P. J., Shields, G. A., & Wheeler, J. C. 1977, ApJ, 212, 367
Zier, C. 2000, Ph.D. Thesis, University of Bonn
Zier, C., & Biermann, P. L. 2001, A&A, 377, 23 (Paper I)